QC
983
A27

JUL 7

MONTHLY WEATHER REVIEW

VOLUME 78 NUMBER 3

MARCH 1950

CONTENTS

		Page
Forecasting Local Showers in Florida During the Summer	Robert C. Gentry	41
The Weather and Circulation of March 1950	Jay S. Winston	50
The Intense Midwest Storm of March 25–27, 1950	Sidney Teweles, Jr., and Lewis C. Norton	52

Charts I–XI

U. S. DEPARTMENT OF COMMERCE · WEATHER BUREAU

UNIVERSITY OF MICHIGAN
GENERAL LIBRARY

NOTICE OF CHANGE IN MONTHLY WEATHER REVIEW

The monthly climatological data tables carried in the Monthly Weather Review through December 1949 now appear in "Climatological Data, National Summary." The subscription price to "Climatological Data, National Summary" is 15 cents per copy or $1.50 per year; remittance (payable to Treasurer of the United States) and correspondence regarding subscriptions should be sent to Superintendent of Documents, Government Printing Office, Washington 25, D. C.

DEPOSITED BY THE
UNITED STATES OF AMERICA

DEPARTMENT OF COMMERCE
CHARLES SAWYER, Secretary

WEATHER BUREAU
F. W. REICHELDERFER, Chief

MONTHLY WEATHER REVIEW

Editor, JAMES E. CASKEY, Jr.

Volume 78
Number 3

MARCH 1950

Closed May 5, 1950
Issued June 15, 1950

FORECASTING LOCAL SHOWERS IN FLORIDA DURING THE SUMMER

ROBERT C. GENTRY
Weather Bureau Office, Miami, Fla.

[Manuscript received April 3, 1950]

ABSTRACT

July and August precipitation records for 5 years from 10 stations within 25 miles of Miami are analyzed to obtain an indication of the frequency of summer showers in that area. Several meteorological parameters for forecasting showers are examined. A quasi-objective method is developed which can be used to forecast the proportion of the Miami area which should expect showers during a 24-hour period 9 to 33 hours in advance. Several parameters are listed which were tested, but did not improve the forecasts. Verification results using independent data are included.

CONTENTS

	Page
Introduction	41
Selection of data	42
Selection of parameters	42
Typing of maps	43
Construction of forecast graphs	44
Type A forecasts	44
Type B forecasts	46
Type C forecasts	46
Modification of basic forecasts	46
Correction rules	46
Other parameters	47
Summary of forecast procedure	48
Tests	48
Conclusions	49
Acknowledgments	49
References	49

INTRODUCTION

Local showers occur so frequently in Florida during the summer that most forecasters give up trying to forecast variations in shower activity and instead put out a standard forecast—"Partly Cloudy with Scattered Showers"—every day, except for the very rare occasion when fair weather is indicated. Although this forecast of partly cloudy with scattered showers will verify for Florida about 90 percent or more of the time, it doesn't give the public much information not already known. As a result, the Florida public consults the weather forecast infrequently during the summer, unless there is a tropical storm. This paper presents an approach to making precipitation forecasts for Florida in the summer months that will have more meaning. It is a pilot project worked out for an area of about 25 miles radius centered around Miami. However, it is hoped that ideas which were found to work for this area will also work, when properly applied, to other sections of the Florida Peninsula.

An examination of climatological data reveals that there is a shower somewhere in Florida almost every day during the summer season. However, the percentage of stations reporting showers during any 24-hour period varies widely from day to day. Data from 10 raingages located near Miami (fig. 1) were compiled for July and August for 5 years. Thus there were data for 310 days. Table 1 gives the frequency that showers were observed during July and August, 1944, 1945, 1947, 1948, and 1949.

TABLE 1.—*Frequency of showers reported by stations near Miami, July and August, 1944, 1945, 1947, 1948, and 1949*

Tenths of stations near Miami reporting rain	Number of days (July and Aug.)	Percent of all days	Percent of days having value or less
0	32	10.3	10
1	28	9.0	19
2	19	6.1	25
3	24	7.7	33
4	31	10.0	43
5	20	6.5	50
6	32	10.3	60
7	35	11.3	71
8	25	8.1	79
9	37	11.9	91
10	27	8.7	100

885753—50——1

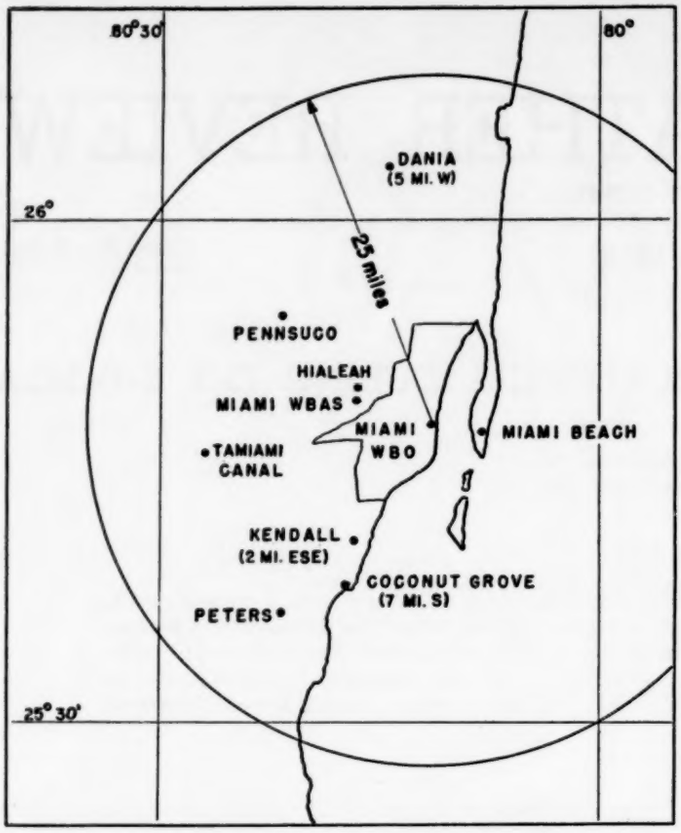

FIGURE 1.—Location of stations near Miami at which precipitation was observed.

During this period, there were almost equal numbers of days in which no stations reported rain, 4 stations reported rain, 10 stations reported rain, etc. The standard forecast of partly cloudy with scattered showers would have verified about 90 percent of the time; and, if it is assumed that some showers occurred without rain falling in any of the 10 raingages, the forecast would have verified over 90 percent of the time. However, data in table 1 show how meangingless is the "standard" forecast. Price [1] has emphasized the usefulness of the probability forecasts of thunderstorms. The present writer believes that Miami forecasts would have more meaning than the "standard" forecast and be of more service to the public if they contained a statement indicating the proportion of the area that was expected to have showers during the period. The forecast procedure explained in this paper is adaptable to that type of forecast.

SELECTION OF DATA

To insure that the precipitation records used in developing the forecast procedure would be representative of the area, data from 10 stations near Miami (fig. 1) were examined and compiled. Some of the stations were operated by cooperative observers of the Weather Bureau, and the rain was measured once a day—usually at about 0800 EST. At the Miami Beach station the accumulated precipitation was measured at about 1700 EST, and during part of the period records were available showing the amount measured at about 0700 EST. At the Miami Airport measurements were made at about 0115, 0715, 1315, and 1915 EST. At stations where recording raingages were used, hourly amounts of precipitation were available. Since raingages do not record traces, a trace was considered as no rain.

Since at several of the stations measurements were made at about 0700 or 0800 EST, it was decided to use a 24-hour period from 0730 EST on 1 day to 0730 EST of the following day. The only station that presented difficulties in using this period was the one at Miami Beach. During the period when records of the 0700 EST measurements were available, its data could be easily adjusted to be approximately concurrent with the others. During the time when 0700 EST measurements were not available, times of occurrence of precipitation were noted at neighboring stations and a decision was made as to which 24-hour period rain measured at 1700 EST should be assigned. Of course this introduces some errors, and the fact that observations at all stations were not made regularly at the same time, i. e., 0730 EST, would introduce some errors. However, it is believed that none of these would be great enough or occur frequently enough to seriously affect any of the results.

Although 10 stations were used in the study, occasionally one or two were missing. For such days the percentage of the remaining stations reporting was computed and that percentage was used.

Data used in making the forecasts were the upper air data observed at about 0330 GMT, and surface data observed at about 0030 GMT. The forecast period was for the 24-hour period beginning at 0730 EST (1230 GMT). Thus the forecast period began about 9 hours after the latest observations were taken. As already noted, this period was chosen because of convenience in handling the precipitation records. However, the forecasting method should work about as well for any other period, because none of the forecast parameters (see p. 44–46) vary very much diurnially with the possible exception of the average relative humidity above Miami.

SELECTION OF PARAMETERS

Following the selection of data for use in developing the forecast procedure, meteorological parameters useful in segregating the days of general showers from those with few or no showers were sought. Since very few air mass changes occur in south Florida in the summertime, one would suspect high correlation between number of showers, and the lapse rate and humidity. An examination of about 150 July and August soundings taken at Miami, however, showed that the lapse rate was always between the wet and dry adiabatic lapse rates. Furthermore, there seemed to be very little correlation between the degree of conditional instability and the number of stations having showers. This agrees with results that Chalker [2]

obtained when studying thunderstorm occurrence throughout the United States. Further analysis of the soundings indicated that percentage of stations reporting rain could not be determined with much accuracy from purely thermodynamic considerations even when the moisture content was also considered. A large group of soundings were analyzed, using both the parcel and slice methods of analysis. Both methods gave consistently poor results. This agrees with studies of the Thunderstorm Project as reported by Byers and Rodebush [3]. They concluded that in each case of widespread thunderstorm activity attributed to insolation in earlier literature there must be a dynamically induced source of low-level convergence, perhaps in some cases related to the diurnal heating. Since high-moisture content through a deep layer results from low-level convergence, that conclusion is in agreement with the well-known correlation between thunderstorm areas and the locations of moist tongues on isentropic or related charts.

From the vorticity theorem [4] it can be argued that horizontal convergence is associated with polar troughs, waves in the easterlies and closed cyclonic circulations. Polar troughs occasionally reach as far south as Miami during July and August, particularly at the 5,000-ft. and 10,000-ft. levels. Also waves in the easterlies affect the Miami vicinity frequently during the average July and August. Infrequently, but at least once almost every summer, closed cyclonic circulations—usually tropical storms—pass near enough to Miami to affect its weather. In addition to these, Byers and Rodebush [3] point out the low-level horizontal convergence which is due to the sea breeze. They maintain that this is particularly effective in Florida which, being a peninsula, has a sea breeze coming onto land from three sides.

Summer air masses over Miami are nearly always conditionally unstable and are usually convectively unstable. There is usually sufficient daytime heating to release any convective instability. The sea breeze blows on most days in July and August, and it should cause enough horizontal convergence near the surface to release the convective instability. For these reasons, it would appear, there should be general showers nearly every day. However, as indicated in table 1, there is a wide variation in the number of stations reporting showers from day to day. The problem then seemed to be (1) to identify general circulation patterns that encourage the release of convective instability and/or bring in moist air during the forecast period, and (2) to identify general circulation patterns which tend to suppress convective instability and/or bring in dry air during the forecast period.

Types of circulation which will usually give horizontal convergence are troughs approaching Miami, easterly waves approaching, cyclonically curved streamlines, and tropical storms. Types of circulations which will usually cause horizontal divergence and thus inhibit ascending motion, are ridges centered right over Miami, strong anticyclonically curved streamlines, and back sides of

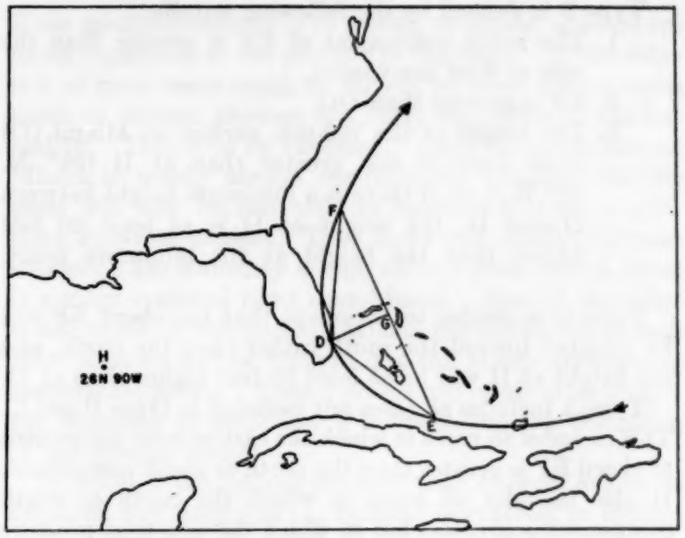

FIGURE 2.—Schematic representation of criteria for typing 700-mb. maps. Point D is at Miami, chords DE and DF are equal to 5° of latitude (25°–30°) and the arc EDF is the 700-mb. contour line.

easterly waves and polar troughs. Any pattern which causes low-level horizontal convergence will probably increase the moisture in air over Miami.

After a number of parameters indicative of the circulation-stability-moisture conditions had been tried, the following were found to be most helpful in segregating the days of general showers from those with few or no showers: (1) the relative humidity, (2) distance from Miami of 700-mb. ridge, (3) degree and type of curvature of 850-mb. and 700-mb. contour lines near Miami, (4) direction and distance of nearest easterly wave, if any, (5) direction and distance from Miami of nearest tropical storm, if any, (6) direction and distance from Miami of nearest polar trough at 700 mb., and (7) general trajectory of air coming to Miami.

TYPING OF MAPS

The next step in developing the forecasting method was to type the 700-mb. maps [1] so that application of the meteorological parameters would be to data for similar synoptic situations. The maps were divided into three types: A—maps of predominantly zonal flow or of weak meridional flow; B—maps of moderate to strong meridional flow with Miami being under the flow from the south; C—maps of moderate to strong meridional flow with Miami being under the flow from the north. Since an effort was being made to make the method objective, definitions were set up to rigidly assign the maps to the respective types. Type B is illustrated in figure 2. Chords DE and DF are each equal to the distance between latitude circles 25 and 30. The point D is at Miami and the arc EDF is the 700-mb. contour line which passes over Miami.

[1] During the period from 1944 to 1949 the Weather Bureau changed from constant level maps to constant pressure maps. For convenience, the map will be called the 700-mb. map or 850-mb. map, etc., even though data from 1944 and 1945 were taken from 10,000-ft. maps or 4,000-ft. maps. (5,000-ft. maps were not easily obtainable for the study, so the 4,000-ft. maps were used instead for July and August, 1944 and 1945.)

Type B is defined by the following criteria:

1. The north component of EF is greater than the east or west component.
2. EF is greater than DG.
3. The height of the 700-mb. surface at Miami (D) is at least 50 feet greater than at H (26° N. 90° W.); or, if there is a minimum height between D and H, the height at D is at least 50 feet higher than the height at the minimum point.

Type C is similar to B, except that the chord EF will be oriented toward the south rather than the north, and the height at H will be at least 50 feet higher than at D.

Type A includes all cases not included in types B and C. This includes all cases in which the east or west component of chord EF is greater than the north or south component. It also includes all cases in which the north or south component is greatest but in which the east-west pressure gradient measured along a line from D to H is weak, or in which the anticyclonic curvature of the contour line from E to F is unusually intense.

CONSTRUCTION OF FORECAST GRAPHS

In developing the forecast method, graphs (scatter diagrams) similar to those given in figures 3–9 were prepared from data for July 1944, 1945, and August 1944, 1945, 1947. Data for July 1947, 1948, 1949, and August 1948 and 1949 were used as independent data to test results presented in the graphs. The graphs in figures 3–9, which give the basic forecasts, were prepared later and include all data both dependent and independent. However, they differ in minor details only from the original graphs. Details of the construction of the graphs for each 700-mb. map type follow.

TYPE A FORECASTS

Most of the maps were type A. The basic forecasts for type A are given in figures 3, 4, and 5. Forecast number 1A (fig. 3) uses average relative humidity as one parameter, entered on the graph as the abscissa. After various humidity measurements had been tried, it was decided that best results were obtained by using an average value. On the forecast charts (figs. 3, 6), relative humidity refers to the average of relative humidity values at 5,000 ft., 10,000 ft., and 15,000 ft. for 1944 and 1945 data, and for the average of humidity values at the 850-mb., 700-mb., and 500-mb. levels for the remainder of the data.

Forecast 1A (fig. 3) uses distance from Miami to the 700-mb. ridge as the second parameter, entered on the graph as the ordinate. If the 10,000-ft. wind at Miami has a westerly component, the ridge used is the one nearest to the south. If the 10,000-ft. wind at Miami has an easterly component, the ridge used is the one nearest to the north. The distance to the ridge line is measured along the meridian passing through Miami in units north or south of Miami. For convenience, a unit of distance equal to 1° of latitude (25° to 26°) was used for the measurements.

On the graph (fig. 3) at the intersection of the abscissa and ordinate values was plotted a number which gives tenths of stations near Miami reporting rain during the 24-hour period. After the data were plotted, isolines were so drawn that the majority of days on one side of a line have values $\geq n$, and the majority of days on the other side have values $< n$, where n is the labeled value of the line.

Forecast 2A (fig. 4) uses parameters which give a measurement of the type and degree of curvature at the 700-mb. and 850-mb. levels near Miami. On each map the contour line that passes over Miami was sketched. Then with Miami as a center and a radius equal to 5 units (5° of latitude) points were marked both upstream and downstream on the Miami contour line, e.g., points E and F in figure 2. Then the line EF was measured and this value was used as a radius of curvature factor. The maximum length of this line is 10. If it was less than 10 and the

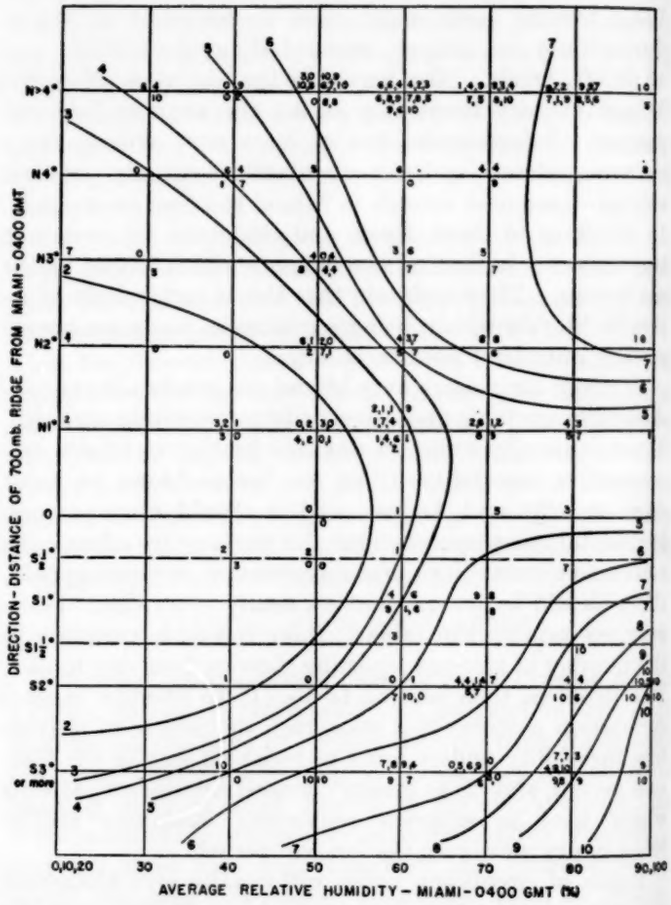

FIGURE 3.—Scatter diagram for type A, forecast 1A. Plotted numbers are tenths of stations near Miami reporting rain in the 24-hr. period 0730–0730 EST. Curves are so drawn that the majority of numbers on one side of a line have values $\geq n$ and the majority of numbers on the other side have values $< n$ where n is the labeled value of the line.

reason for its being less was cyclonic curvature of the contour lines, then radius of curvature factor was classed as cyclonic. It is possible for the curvature at Miami to be cyclonic and for the general curvature over the length of 10 units to be anticyclonic. It is the value for the entire 10 units which was considered in arriving at classification of the curvature. Admittedly this is somewhat arbitrary, but examination of maps in the series showed that it gave slightly more reliable results than taking the curvature at Miami.

If length of EF was less than 10 and curvature was anticyclonic, EF was measured and the value recorded as the radius of curvature factor. Values of this factor for 850-mb. and 700-mb. maps were used as coordinates in plotting figure 4. Values at the coordinate intersections are tenths of stations near Miami reporting rain. Isolines were drawn on this chart as in figure 3. Thus we have two forecasts for type A. These forecasts, 1A and 2A (figs. 3 and 4), were used in plotting figure 5 and isolines were drawn as before. Forecast 3A (fig. 5) is the basic forecast for type A.

Figure 3 shows that for type A situations showers are unlikely if the humidity is 50 percent or less and the 700-mb. ridge is within 2 units north or south of Miami. If the relative humidity is 70 percent or higher, showers are likely regardless of the position of the ridge. If the ridge is 3 or more units south of Miami, or more than 4 units north of Miami, showers are likely regardless of the humidity. This is to be expected. Since the lapse rate at Miami is nearly always conditionally unstable, the air mass will also be convectively unstable if there is sufficient moisture present. Thus there will usually be some showers if the humidity is high enough even though there is a ridge centered right over Miami. Also, if the ridge is well north or well south of Miami, the circulation is such that moist air will be brought into the Miami area during the forecast period. Thus showers will result even though the humidity is quite low 9 hours before the beginning of the forecast period.

In figure 4 the isolines indicate that showers are to be expected any time there is cyclonic curvature, as defined and measured in the radius of curvature factor, either at 850 mb. or 700 mb. Also there will usually be showers if the contour lines are curved slightly anticyclonically. However, if the contour lines at either level are curved sharply anticyclonically, there is reduced chance for showers; and if they are curved sharply anticyclonically at both levels, there is very little chance for showers.

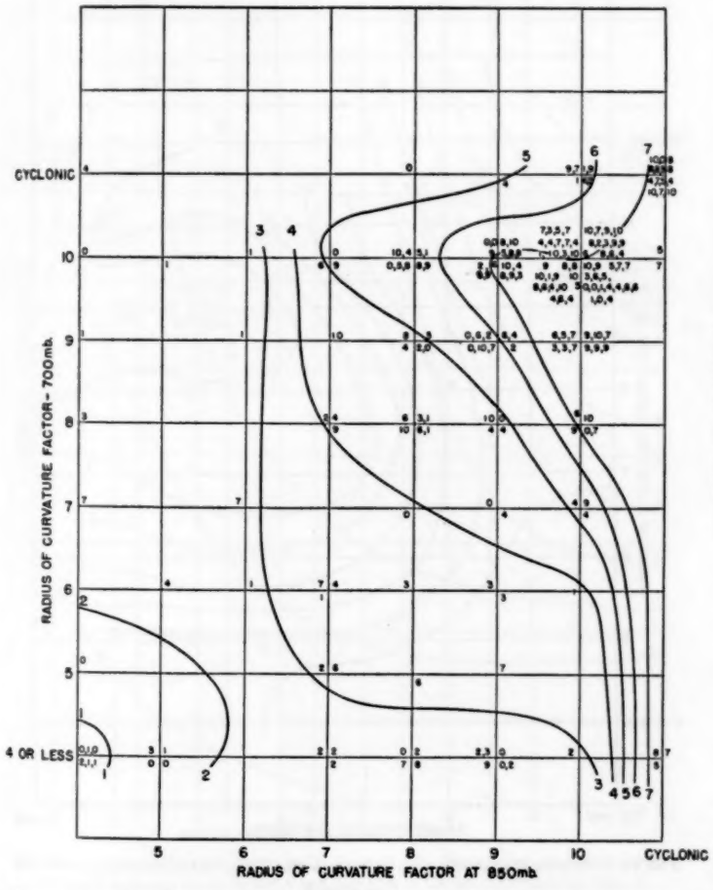

FIGURE 4.—Scatter diagram for type A, forecast 2A. Graph is constructed in same way as figure 3.

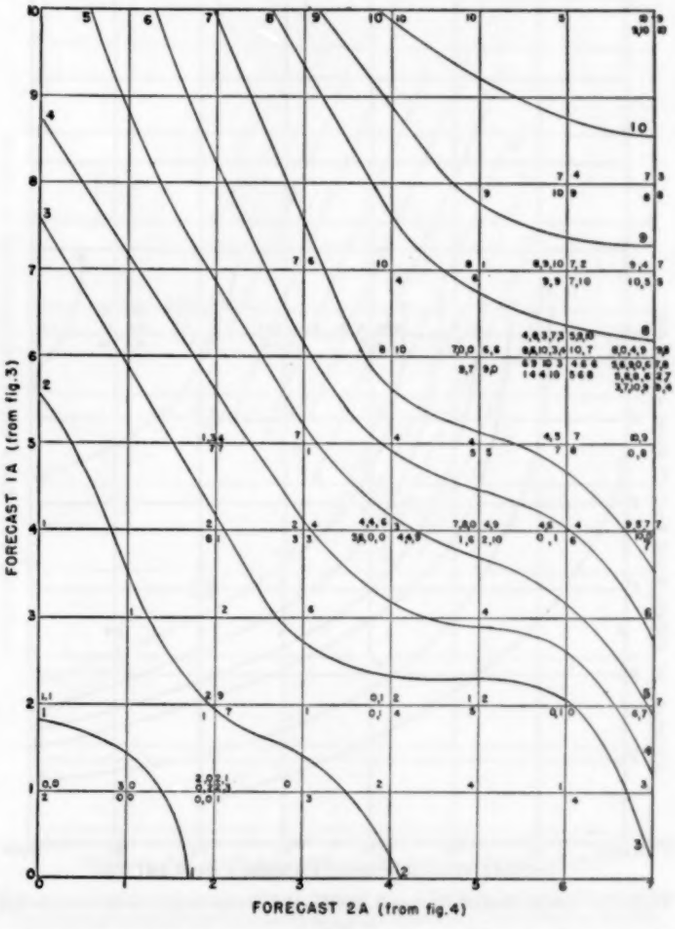

FIGURE 5.—Scatter diagram for type A, forecast 3A. Parameters used here are the forecasts obtained from curves in figures 3 and 4. This is the basic forecast for type A.

TYPE B FORECASTS

Forecast graphs for type B given in figures 6, 7, and 8 were made in a fashion similar to those for type A, except that distance to the ridge was measured along the latitude circle passing through Miami and was measured only to the east.

Similar conclusions to those for type A can be drawn for type B maps after a study of figures 6 and 7. Showers are more frequent when the humidity is high and when the ridge is several units distant from Miami. Type B as a whole is more showery than type A; so showers occur on almost all days except when the relative humidity is very low or when the ridge is within 4 units of Miami.

The radius of curvature factor has about the same effect on type B cases as on type A. Showers are frequent when the factor gives cyclonic curvature or when the anticyclonic curvature is slight. Chances for showers get progressively less with increase in the intensity of the anticyclonic curvature, i. e., decrease in the radius of curvature factor.

TYPE C FORECASTS

Forecasts for type C used a parameter not used in the type A and B forecasts. With Miami as the center, and a radius of 5 units, a mark was made upstream on the 700-mb. contour line passing over Miami. Another mark was made 10 units upstream. The longitude at each of these marks was read and the values averaged. The average value is the quantity used as the ordinate in forecast 1C (fig. 9). There were very few cases of type C, so reliability of the forecast 1C is somewhat doubtful. However, figure 9 indicates more probability of rain when the humidity is high and when the average trajectory estimated by the longitude factor is such as to have brought the air over water for a long distance before it reaches Miami. This seems logical and agrees with observations of experienced meteorologists.

MODIFICATION OF BASIC FORECASTS

CORRECTION RULES

Some other parameters were tested and found to improve the basic forecasts given in figures 5, 8, and 9. These other parameters do not occur every day. In fact, there were insufficient cases to justify drawing additional graphs. It was believed that about as good results could be obtained by stating them in forecast rules as corrections of the basic forecasts. Perhaps when additional data have been studied there will be sufficient cases to justify

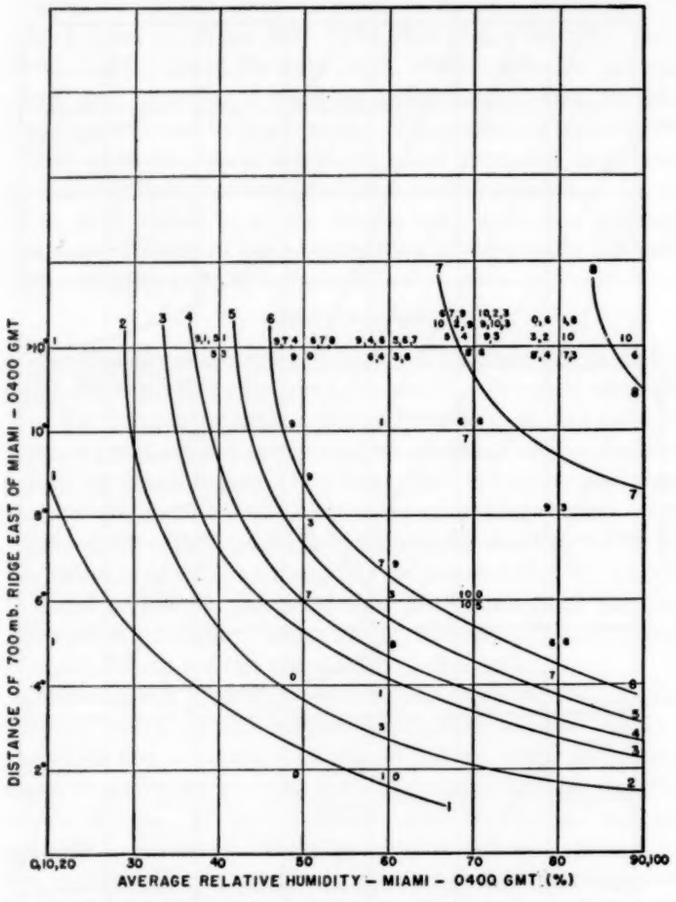

FIGURE 6.—Scatter diagram for type B, forecast 1B. Graph is constructed in same way as figure 3.

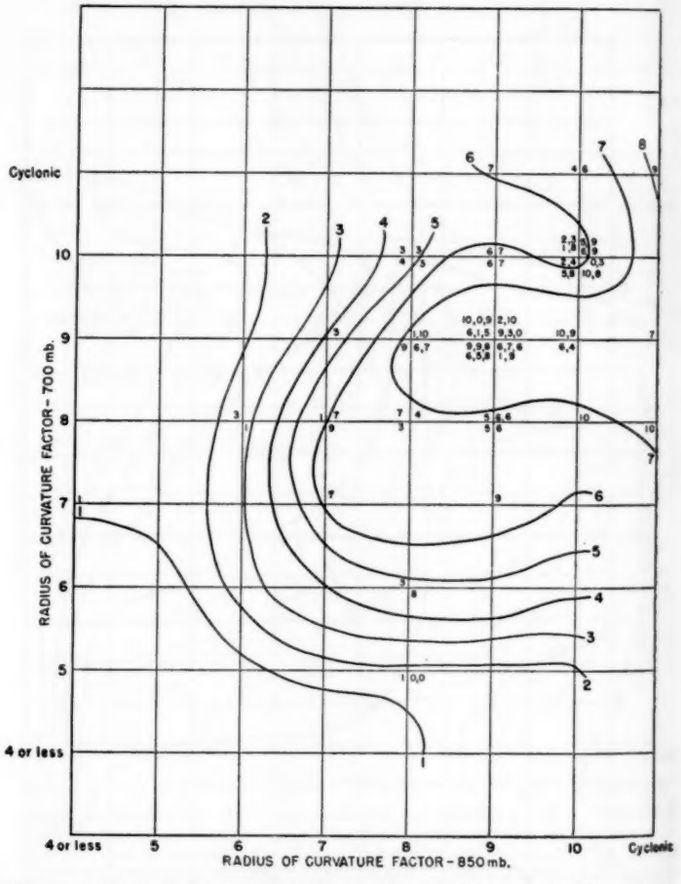

FIGURE 7.—Scatter diagram for type B, forecast 2B. Graph is constructed in same way as figure 3.

drawing additional graphs and preparing more accurate solutions. These rules are based partially on results found in studying the dependent data and partially on experience of the Miami forecasters. They are stated as corrections to the basic forecasts given in figures 5, 8, and 9. The rules follow:

(1) If there is an easterly wave at 2,000 ft. whose axis is located within 2 units to the west of Miami or within 6 units (1 unit equals 1 degree of latitude) to the east of Miami, add one-tenth to the basic forecast. (See Dunn [5] for a discussion of easterly waves.)

(2) If there is an easterly wave at 2,000 ft. whose axis is located within 4 to 8 units to the west of Miami, subtract two-tenths from the basic forecast.

(3) If there is an easterly wave at 2,000 ft. whose axis is within 2 to 6 units to the north or northwest of Miami, subtract two-tenths from the basic forecast.

(4) If Miami is in the westerlies at 700 mb. and there is a trough over Miami or within 10 units to the west, add one-tenth to the basic forecast.

(5) If Miami is in the westerlies at 700 mb. and there is a trough within 5 units to the northwest or 4 units to the north, add one-tenth to the basic forecast.

(6) If Miami is in the westerlies at 700 mb. and there is a trough 3 or 4 units to the east, subtract two-tenths from the basic forecast.

(7) When at 10,000 ft. there is a shear line north of Melbourne and the 10,000-ft. wind at Tallahassee is on or between ESE and ENE, subtract two-tenths from the basic forecast (fig. 10). Do not use this rule for those cases in which the streamline or contour line is curved cyclonically continuously from Miami to Tallahassee.

(8) If there is a tropical storm in areas X or Y (fig. 11), subtract the number of tenths indicated on the map.

OTHER PARAMETERS

Many other parameters were tried and found to have either little correlation with the number of showers or such a high correlation with the parameters already used in forming the basic forecasts that they added little or nothing to the skill. A list of these follows:

1. Sign of the curvature of the 850-mb. and 700-mb. contour lines at Miami.
2. Occurrence of precipitation up wind 12–18 hours preceding the forecast period.

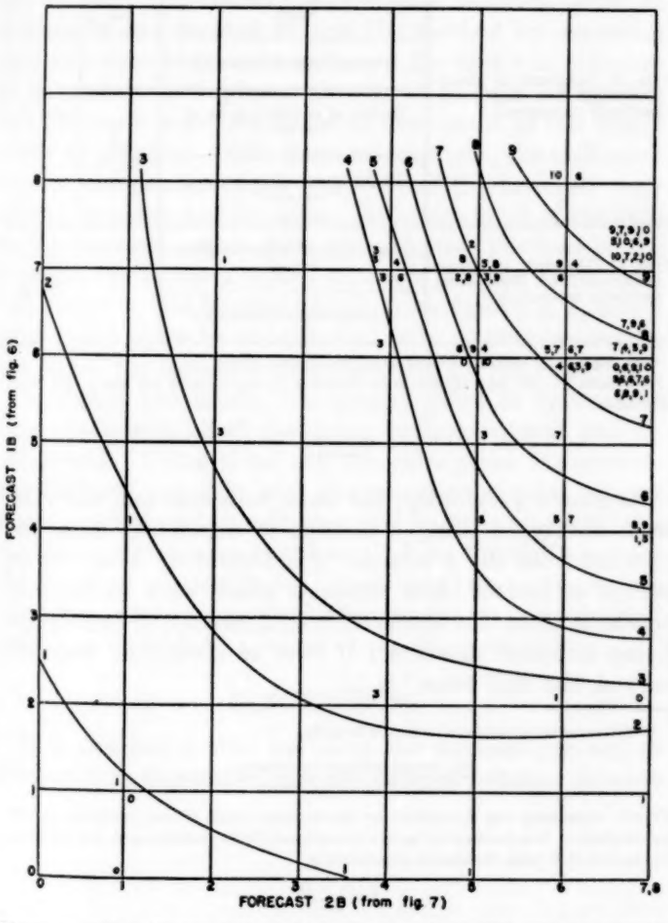

FIGURE 8.—Scatter diagram for type B, forecast 3B. Parameters used are forecasts obtained from curves in figures 6 and 7. This is the basic forecast for type B.

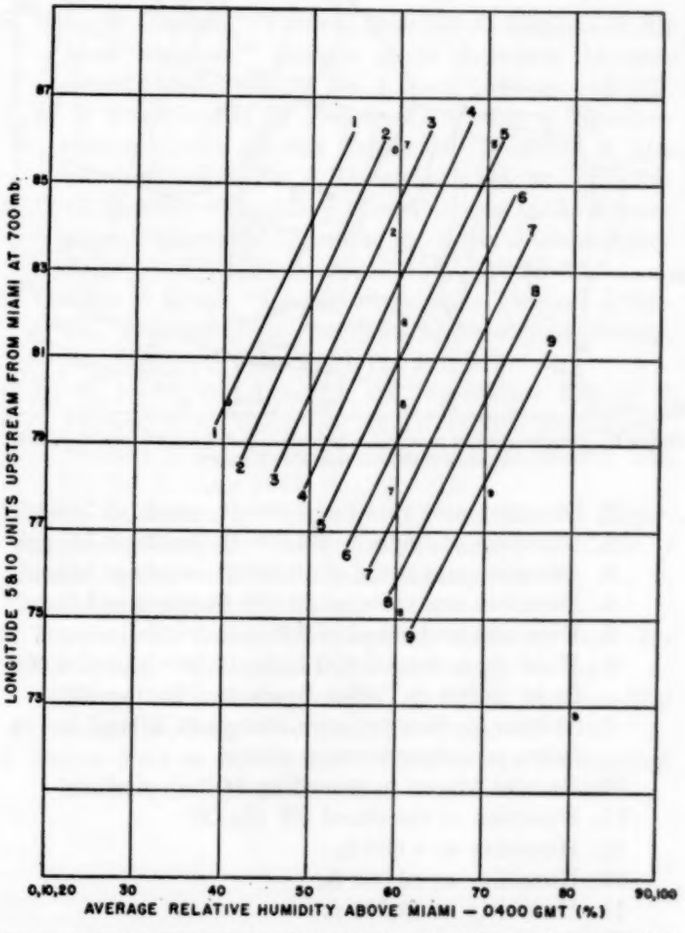

FIGURE 9.—Scatter diagram for type C, forecast 1C. The ordinate is the average of the two values of longitude read at points 5 and 10 units upstream from Miami at 10,000 ft.

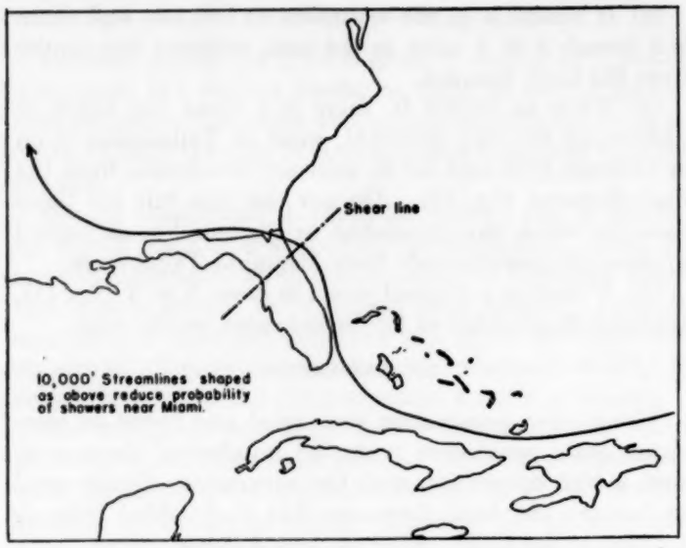

FIGURE 10.—Schematic representation of rule number 7.

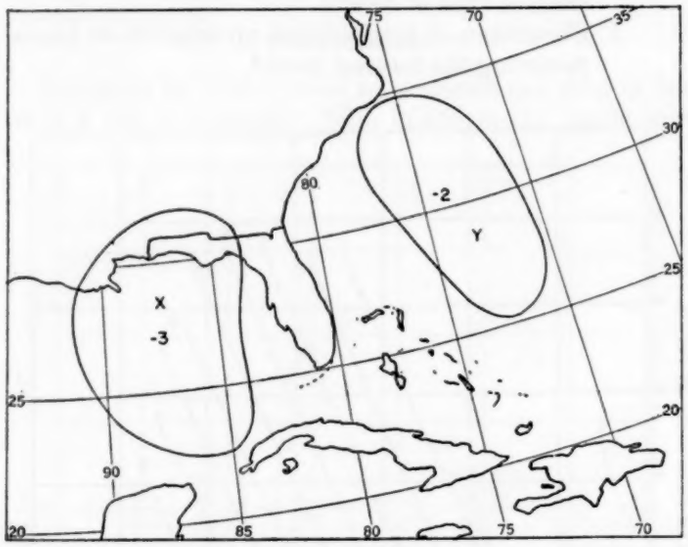

FIGURE 11.—Diagram showing correction to be made to basic forecast if tropical storm is centered in either of areas X or Y (rule 8).

3. Direction and speed of 2,000-ft. winds at Miami.
4. Direction and speed of 5,000-ft. winds at Miami.
5. Direction and speed of 10,000-ft. winds at Miami.
6. Direction and speed of 20,000-ft. winds at Miami.
7. Direction and speed of 8,000-ft. winds.
8. Wind shear from 2,000 ft. to 10,000 ft. and 5,000 ft. to 10,000 ft. (See Byers and Battan [6].)
9. 24-hour surface pressure change at Miami for 24 hours preceding forecast period.
10. Rain at Miami in preceding 24-hour period.
11. Direction of the chord EF (fig. 2).
12. Humidity at 5,000 ft.
13. Humidity at 10,000 ft.
14. Humidity at 15,000 ft.
15. Humidity at 20,000 ft.
16. Convergence in wind field over area immediately preceding forecast period. (Computed for a few cases only by a method developed by Bellamy [7].)
17. Instability as computed by slice method [8].
18. Instability as computed by parcel method [9].

SUMMARY OF FORECAST PROCEDURE

The forecast procedure which has been developed is summarized schematically in table 2.

TABLE 2.—*Summary of forecast procedure*

Type	Parameters	Forecasts [1]	
Type A (Zonal flow at 700 mb. or weak meridional flow).[1]	Distance to 700-mb. ridge.	1A (fig. 3)	3A (fig. 5)
	Average relative humidity.		
	Radius of curvature factor at 700 mb.	2A (fig. 4)	
	Radius of curvature factor at 850 mb.		
Type B (Moderate to strong meridional flow from some southerly component).[1]	Distance eastward to 700-mb. ridge.	1B (fig. 6)	3B (fig. 8)
	Average relative humidity		
	Radius of curvature factor at 700 mb.	2B (fig. 7)	
	Radius of curvature factor at 850 mb.		
Type C (Moderate to strong meridional flow from some northerly component).[1]	700-mb. air trajectory (longitude factor).		1C (fig. 9)
	Average relative humidity.		

[1] See pages 43 for detailed criteria for typing 700-mb. maps.

[2] Forecasts 3A, 3B, and 1C are to be modified by use of rules 1–8 (see p. 47) when applicable.

TESTS

As stated previously, the basic forecasts and the rules were developed using 5 months of dependent data and checked with the 5 months of independent data. If we accept as correct those forecasts which were within two-tenths of what was observed, i. e., a forecast of four-tenths being accepted as correct if two- to six-tenths were observed, the skill score [2] is 55.

[2] Skill scores were computed from the formula

$$S = \frac{\text{No. correct} - \text{chance expectancy}}{\text{Total} - \text{chance expectancy}} \times 100$$

Chance expectancy was determined by the marginal totals of both predicted and observed classes. In a contingency table with subtotals P_i for predicted and O_i for observed and a total of N cases, the chance expectancy is

$$\frac{\Sigma (P_i \times O_i)}{N}$$

Table 3 gives the number of days of independent data for which the forecasts were exactly correct, the number and percentage of days that were within one-tenth of the observed, the number and percentage of days that were within two-tenths of the observed, etc. The eight-step error and all of the seven-step errors except one were cases in which frequent showers had been forecast and few or none occurred.

TABLE 3.—*Tabulation of number and percentage of days with various step errors in forecasting from independent data*

Step errors in forecasts (tenths)	Number of days	Percentage of days having this error or less
0	41	26
1	38	51
2	36	74
3	14	83
4	8	88
5	9	94
6	2	96
7	6	99
8	1	100
9	0	100
10	0	100

If it is desired not to make forecasts in terms of tenths or percentage, but to forecast either showers or no showers, the method can still be used. Since showers occur so frequently, we decided to test the method by assuming that any time two-tenths or less of the area was expected to have showers to give a forecast of no rain. Likewise, in verifying it was assumed that two-tenths or less would verify as no rain. With these assumptions, the skill score for the independent data was 57, and the forecasts were correct 86 percent of the time. Although most of the skill in the forecasts comes from the objective portions of the method, the forecast rules 1 through 8 added some skill. For example, the forecasts made from figures 5, 8, and 9 gave a skill score for independent data of 47 compared to the 57 for the forecasts when modified by the rules.

As stated previously, the graphs given in figures 3–9 were made with all of the data—both dependent and independent. Using them and the rules given for correcting the basic forecasts, with the exception of rules number 4 and 5 which didn't add any skill to forecasts made by the charts which were based on all data, the skill score for the two-step errors was 58. Assuming two-tenths or less as no rain, and forecasting either rain or no rain, the skill score was 63 with 87 percent of the forecasts correct.

CONCLUSIONS

It is concluded that by using the forecast procedures developed in this paper, one can forecast summer showers in Florida with a high degree of accuracy. It is not necessary to forecast, "Partly Cloudy with Scattered Showers" for southern Florida almost every day in the summer. The forecaster can give the public much more information by predicting what percentage of the area will have showers during the period, and he can do it with considerable accuracy.

ACKNOWLEDGMENTS

The author is grateful to Mr. Grady Norton, Official-in-Charge, Miami Weather Bureau Office, for encouragement and many helpful suggestions offered during the preparation of this paper. Also thanks are due Mr. George Collins and Miss Evelyn Perlich for preparing the figures and the manuscript; and to Mr. Collins, Mr. Charles Gardner, Mrs. Margaret Moore, Mr. Howard Ellis, Mrs. Philo Gwin, and Miss Martha Coster, all of the Miami Weather Bureau, for assistance with the statistical and clerical work.

REFERENCES

1. Saul Price, "Thunderstorm Today?—Try a Probability Forecast," *Weatherwise*, vol. 2, No. 3, June 1949, pp. 61–63.
2. Wm. R. Chalker, "Vertical Stability in Regions of Air Mass Showers," *Bulletin of the American Meteorological Society*, vol. 30, No. 4, April 1949, pp. 145–147.
3. H. R. Byers and H. R. Rodebush, "Causes of Thunderstorms of the Florida Peninsula," *Journal of Meteorology*, vol. 5, No. 6, December 1948, pp. 275–280.
4. C.-G. Rossby, "Planetary Flow Patterns in the Atmosphere," *Quarterly Journal of the Royal Meteorological Society*, vol. 66, Supplement, 1940, pp. 68–87.
5. Gordon E. Dunn, "Cyclogenesis in the Tropical Atlantic," *Bulletin of the American Meteorological Society*, vol. 21, No. 6, June 1940, pp. 215–217.
6. H. R. Byers and Louis J. Battan, "Some Effects of Vertical Wind Shear on Thunderstorm Structure," *Bulletin of the American Meteorological Society*, vol. 30, No. 5, May 1949, pp. 168–175.
7. John C. Bellamy, "Objective Calculations of Divergence, Vertical Velocity and Vorticity," *Bulletin of the American Meteorological Society*, vol. 30, No. 2, February 1949, pp. 45–49.
8. Norman R. Beers "Atmospheric Stability and Instability" in *Handbook of Meteorology*, ed. by F. A. Berry, Jr., E. Bollay, and N. R. Beers, McGraw-Hill Book Co., Inc., New York, 1940, pp. 693–725.
9. Sverre Petterssen, *Weather Analysis and Forecasting*, McGraw-Hill Book Co. Inc., New York, 1940.

THE WEATHER AND CIRCULATION OF MARCH 1950 [1]

JAY S. WINSTON

Extended Forecast Section, U. S. Weather Bureau,
Washington, D. C.

The atmospheric circulation over the Pacific, North America, and the Atlantic during March 1950 was characterized by three zonal belts of 700-mb. height anomaly, negative at middle latitudes (35° to 55° N.) and positive at higher and lower latitudes (see fig. 1). Consequently, westerly winds were considerably stronger than normal between latitudes 30° and 45° N. and weaker than normal between 50° and 60° N. In figure 2 the geostrophic zonal wind speed profile for March 1950 is shown in comparison with the normal profile for March for the Western Hemisphere (0° to 180°). It can be seen that the speeds in the mean jet stream for March 1950 exceeded the normal by as much as 5 m/sec, and the jet was displaced somewhat to the south of the normal.

Returning to figure 1 it is evident that the subpolar lows in the Aleutians and in eastern North America were displaced well to the south of their normal positions and the broad cyclonic circulations associated with them covered extensive areas at middle and lower latitudes. At higher latitudes a large warm ridge covered much of the Arctic Ocean and northern Canada while anticyclonic conditions were also well developed from Greenland into western Europe. The high centered in northwestern Canada was apparently associated with one that had appeared on monthly mean charts over the Bering Sea in February and in the eastern Pacific in January (see

[1] See Charts I–XI, following p. 57, for analyzed climatological data for the month.

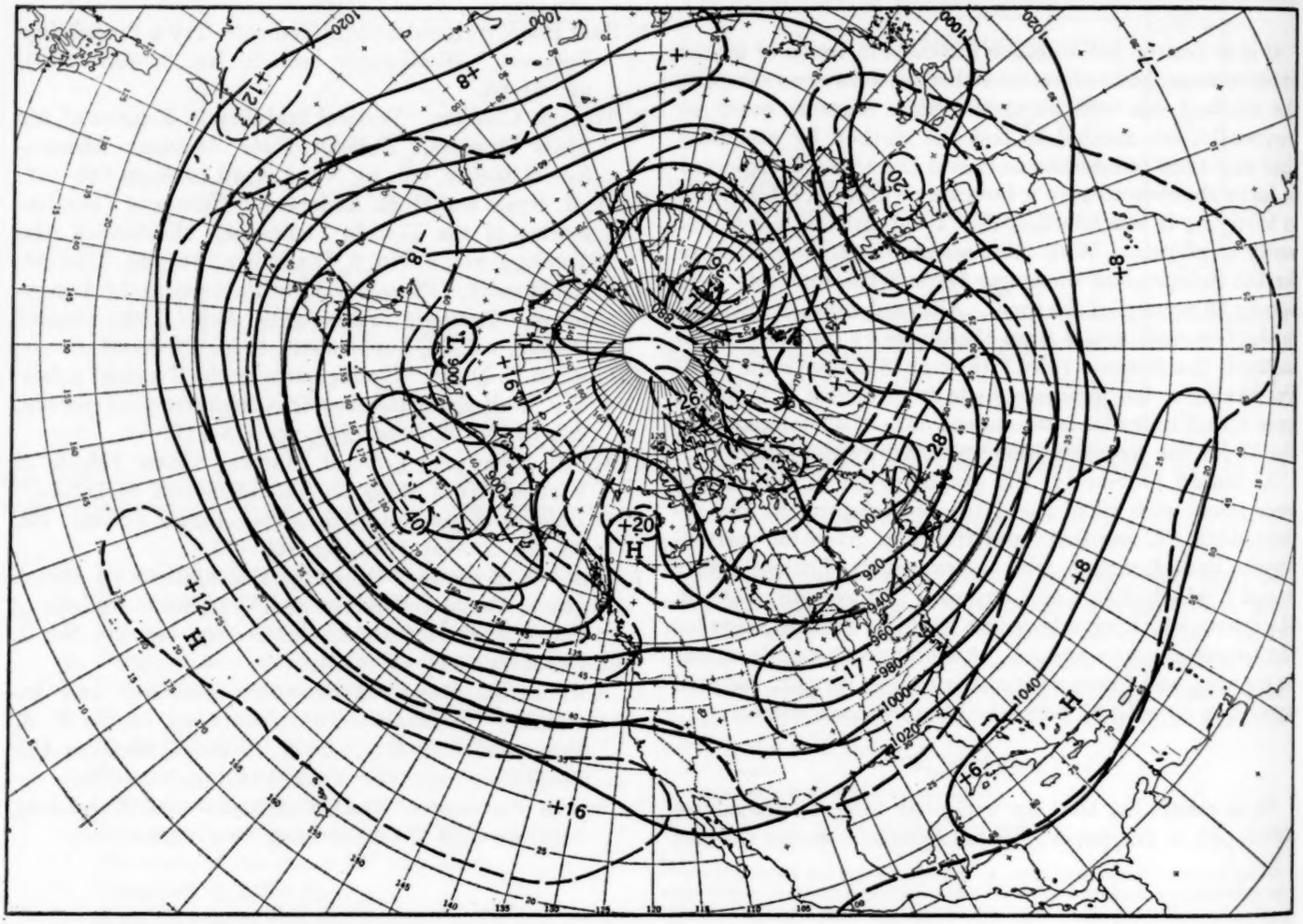

FIGURE 1.—Mean 700-mb. chart for the 30-day period February 28–March 29, 1950, inclusive. Contours at 200-foot intervals are shown by solid lines, 700-mb. height departure from normal at 100-foot intervals by dashed lines, with the zero isopleth heavier. Anomaly centers and contours are labeled in 10's of feet.

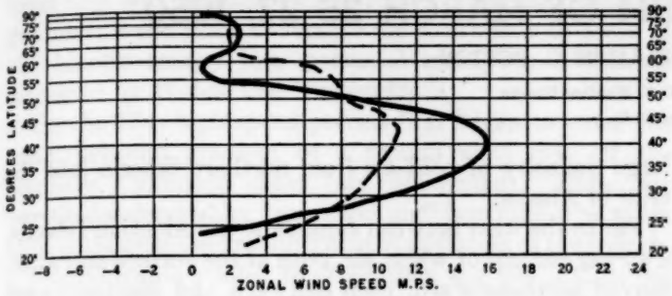

FIGURE 2.—Monthly mean 700-mb. geostrophic zonal wind speed profile in meters per second averaged from 0° westward to 180° longitude. Solid curve is for March 1950, dashed line is March normal.

fig. 1 of the articles by Klein in January 1950 and February 1950 Monthly Weather Reviews). This continuity, which was well established by the intervening midmonth charts (not published), is one of the most remarkable ever observed on monthly mean 700-mb. charts.

This abnormally strong ridge in northwestern Canada combined with the below-normal 700-mb. heights over the greater portion of the United States led to frequent outbreaks of cold Canadian polar air into the northern, central, and eastern United States. Meanwhile, the influence of maritime tropical air was restricted by fast westerlies over southern sections of the United States near the Gulf of Mexico. These considerations explain the subnormal surface temperatures covering practically all of the country east of the Rockies and the northwestern border states as shown in Chart I. The above-normal temperatures in the Great Basin were associated with above-normal heights and anticyclonic conditions at 700 mb. over that area. The warm temperatures in west Texas could be attributed to the foehn effect, since the flow to the east of the Continental Divide in that section was faster than normal.

The tracks of centers of anticyclones given in Chart II show how predominant the polar continental anticyclones were over the eastern two-thirds of the United States during the month. These highs were generally steered by the mean 700-mb. circulation, several of them penetrating far into the South. It is noteworthy that most of these anticyclone centers left the east coast south of the Canadian border (contrast with Chart II for January 1950).

Chart V (inset) shows that heavy precipitation was largely confined to the northern border States and to portions of the eastern third of the country. The major cyclone track (see Chart III) along and south of the United States-Canadian border was responsible for this heavy precipitation stretching from coast to coast in the north. These daily cyclones traveled mainly through the zonal belt of negative height anomaly across the United States, generally steered by the monthly mean 700-mb. circulation. Cyclogenesis was frequent in the central Plains States under the cyclonic curvature and negative center of height anomaly aloft (see fig. 1). Another seat of cyclogenesis, also associated with negative height anomalies at 700 mb., appeared near the east coast of the United States. These cyclones were responsible for heavy precipitation along the east coast. The deficiency of precipitation over much of the Great Basin was associated with ridge conditions aloft and infrequent cyclonic activity in the area. Dry weather also prevailed over the central and southern Plains States since the predominantly northwesterly flow aloft allowed very little advection of maritime tropical air northward into this region.

THE INTENSE MIDWEST STORM OF MARCH 25–27, 1950

SIDNEY TEWELES, JR., AND LEWIS C. NORTON

WBAN Analysis Center, U. S. Weather Bureau,
Washington, D. C.

INTRODUCTION

Severe weather, ranging from dust storms and sandstorms in New Mexico and west Texas to blizzards in the Dakotas, prevailed in the northern Plains area and on the east slope of the Rockies on March 25–27, 1950. These conditions were accompanied by a Low which deepened very rapidly in eastern Colorado and western Nebraska on the 25th and which further intensified as it continued a general north-northeastward course into the Dakotas and Minnesota. At many locations, passage of the Low resulted in the lowest pressure of record.

It is of interest from a synoptic standpoint to examine not only conditions when the storm was most active, but also to investigate some of the causes and effects leading up to the most intense development. To do this requires a study of synoptic conditions for several days in advance and for an area extending some thousands of miles from the region of severe weather.

PRECEDENT SYNOPTIC CONDITIONS

On March 21 a deepening surface wave about 300 miles south of the Aleutian Islands moved rapidly eastward and at 1330 EST on the 22d (fig. 1) the resulting Low, then occluded, was centered at 48° N., 146° W. At that time it had its lowest central pressure, 980 mb., and thereafter decelerated and slowly filled, the occluded front and warm sector becoming dissociated from the low pressure center. The circulation of this Low resulted in the movement of a large quantity of cold air from northern Siberia into the Gulf of Alaska.

Far to the west between Japan and the Aleutian Islands, a strong current of warm air, both at the surface and aloft, moved northeastward, then eastward and southeastward into close contact with the cold air current which was nearer the center of the Gulf of Alaska Low. This confluence of differing currents produced a strong temperature gradient at intermediate levels along the western and southwestern boundary of the cold air, and a resulting strong northwesterly thermal wind component became established over the northerly surface winds which appear near longitude 155° W. in figure 1 and longitude 135° W. in figure 2. The existence of such a large thermal wind component required very strong northwesterly winds aloft. The confluence of upper level warm and cold air currents, and the resulting strong temperature gradient aloft, have been advanced by Namias and Clapp [1] as "ssential features in their theory of the formation of the ejet stream." Figure 3 shows the resulting strong northwesterly current at 500 mb. off the west coast of North America at 2200 EST, March 24. This figure also shows the great amplitude of the isotherm pattern, with temperatures of −15° C. over the stationary ship at 50° N., 145° W., and −30° C. over northern California. In addition, the thermal wind component indicated by the isotherm field in the vicinity of 40° N., 130° W., required that winds between the 500- and 300-mb. levels in that region be even stronger and more northerly. This strong upper

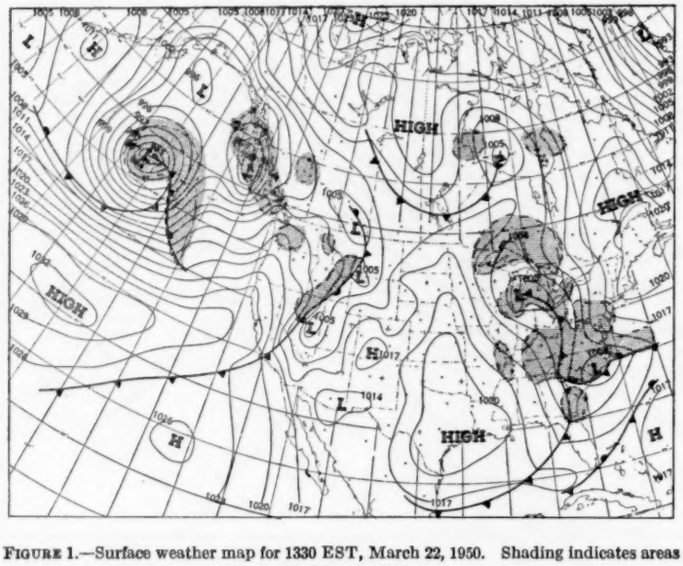

FIGURE 1.—Surface weather map for 1330 EST, March 22, 1950. Shading indicates areas of active precipitation.

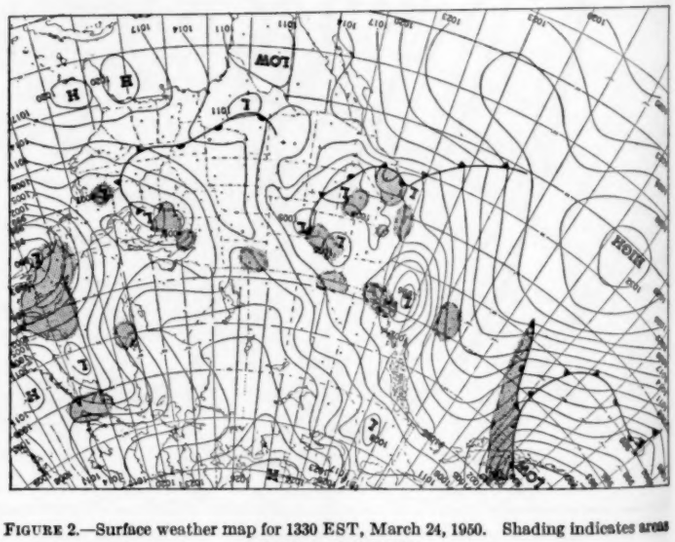

FIGURE 2.—Surface weather map for 1330 EST, March 24, 1950. Shading indicates areas of active precipitation.

level flow was directed into a region of weaker pressure gradient, a condition favorable for conversion of some of the kinetic energy into potential energy in a manner discussed by Wobus and Norton [2].

On the 23d, high speed parcels first began to enter the weak pressure gradient of a trough aloft just off the southern California coast (not illustrated). These air parcels decelerated by "overshooting" into higher pressure with consequent sharpening and retardation of the trough, a process which tended to strengthen the gradient in the portion of the trough near the 30th parallel. After the gradient in the southern portion of the trough had increased, high speed parcels entering that portion of the trough were able to pass through to the east with undiminished speed. Figure 3, for the 500-mb. level, 2200 EST, March 24, shows the trough at this stage of development.

Intensification of the trough in its southern portion was accompanied by a large drop in the height of the 500-mb. surface along the California coast, and the reflection of this pressure drop is found at sea level in the sudden development of a frontal wave, which at 1330 EST, March 24 (fig. 2), was just southwest of San Francisco. Within 12 hours this wave deepened 15 mb. and moved rapidly into Utah, where it was centered at 0130 EST of the 25th (fig. 4).

TEMPERATURE CHANGES ALOFT

Figure 5 shows the soundings at Ely, Nev., for 1000 EST and 2200 EST of the 24th. At both times Ely was very close to the front. However, the wave had approached to within 50 miles of Ely by 2200 EST of the 24th so that these soundings reveal the levels in the atmosphere responsible for the 12-hour pressure fall over Nevada. Comparison of the two soundings shows a slight net cooling from the ground up to 260 mb. The layer between 260 and 100 mb. was appreciably warmer and lighter at the end of the 12-hour period. This marked high level warming was sufficient to compensate for an increase of pressures at heights above the 100-mb. level and the slight net cooling below 260 mb., and in addition, to account for a drop of 6 mb. in station pressure (7.5 mb. in pressure as reduced to sea level). Most of the warming in the high levels above Ely can be explained by advection from the west and northwest. But, as the trough aloft moved over Nevada by the evening of the 25th, the 200-mb. chart showed warm air of greater extent and of higher temperature than any which could have moved into that region by purely horizontal advection from the west and northwest. Therefore, it is probable that adiabatic warming also occurred as air in the upper levels was drawn downward by horizontal divergence at intermediate levels. This horizontal divergence in turn can be accounted for if the strong winds at 500 mb., as illustrated in figure 3 where wind speeds are near 100 knots at San Diego and Tucson, had a cross-isobar component toward higher pressure. Such cross-isobar flow, accompanying an adjustment of pressure gradient as strong winds were injected into the region south of Nevada, appears to have been a factor in drawing air out of the intermediate levels over Nevada.

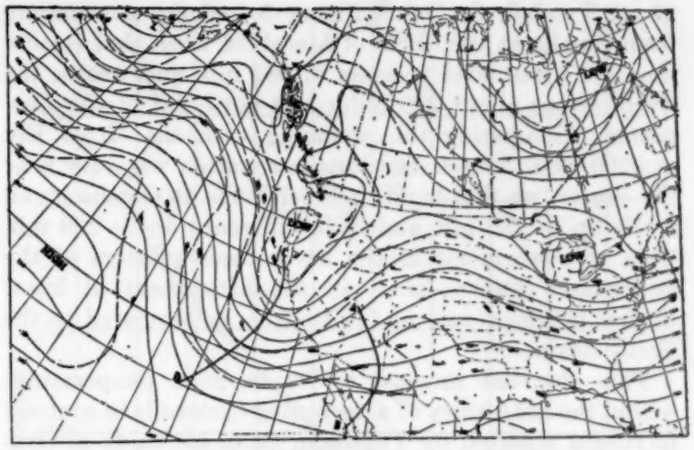

FIGURE 3.—500-mb. chart for 2200 EST, March 24, 1950. Contours (solid lines) at 200-ft. intervals are labeled in hundreds of geopotential feet. Isotherms (dashed lines) are drawn for intervals of 5° C. Winds are plotted in Beaufort scale.

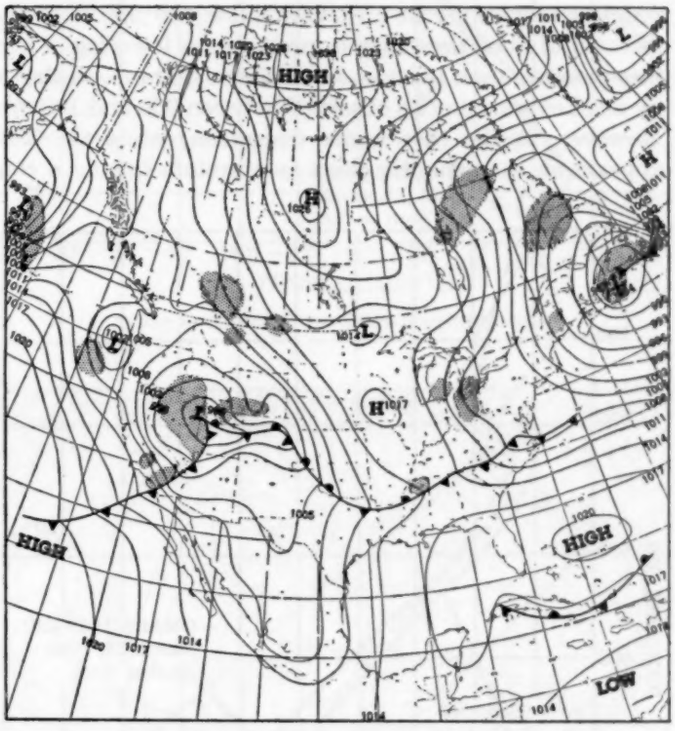

FIGURE 4.—Surface weather map for 0130 EST, March 25, 1950. Shading indicates areas of active precipitation.

The lowest sea level pressure attained by the Low before it redeveloped east of the Continental Divide was near 990 mb. in the vicinity of Salt Lake City, Utah. The lowest pressure reported in the Low after redevelopment east of the Divide was 968 mb. at 0130 EST, March

27 at Tyndall, S. Dak. Figure 5 includes a sounding from Omaha at 1000 EST of March 26 when that station reported a sea level pressure of 982 mb. and was in the warm sector about 200 miles east-northeast of the Low center. Comparing this sounding with that from Ely at 2200 EST, March 24 when that station was very near the center, we find higher temperatures at Omaha at all levels up to 250 mb. and little difference above 250 mb. This very warm air in the lower three-quarters of the atmosphere was a factor in the attainment of lower central pressures east of the Rockies as compared to the Great Basin.

This observed increase of tropospheric temperatures within the life history of a deepening cyclone is in contrast to results reported by Vederman [3] in his study of temperature changes aloft over 25 Lows in the United States *east of the Rockies*, all of which deepened 10 millibars or more. Vederman found in almost all cases, as a Low deepened, the air column over the moving center became progressively cooler at all levels below 400 mb., and the removal of mass necessary to produce the lowering of surface pressure took place at levels above 400 mb. as shown by marked warming he observed between 300 and 100 mb. However, in the case under discussion, while the Low appears on the synoptic chart as a system having a continuous movement across the Plateau and into the Plains area, its rapid deepening along the east slope of the Rockies was in effect a new development, involving a new and warmer air mass which was not present over the Plateau. Warming of the troposphere over the Low center was therefore associated with transformation of the system from a Plateau Low to a Plains Low. Further deepening as the Low moved through the northern Plains was accompanied by cooling of the troposphere over the moving center, in agreement with Vederman's results.

The high temperatures attained below 700 mb. may be seen by comparing the thickness charts in figures 6 and 7. These charts show the difference in height between the 1000-mb. and 700-mb. levels, and since a given thickness corresponds to a fixed value of mean virtual temperature between the levels, the lines are labeled in degrees Centigrade at one end and thickness, in geopotential feet, on the other end. The large arrows with hollow heads show the flow of air at 850 mb. from warm to cold areas and indicate, in a qualitative manner, the areas where warm advection is taking place. In an analogous fashion, the

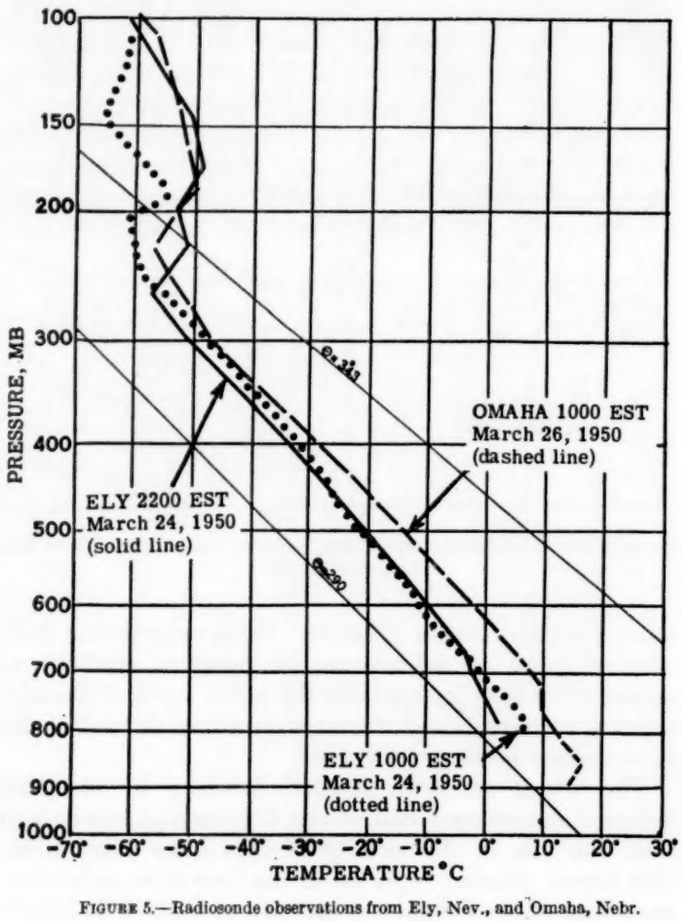

FIGURE 5.—Radiosonde observations from Ely, Nev., and Omaha, Nebr.

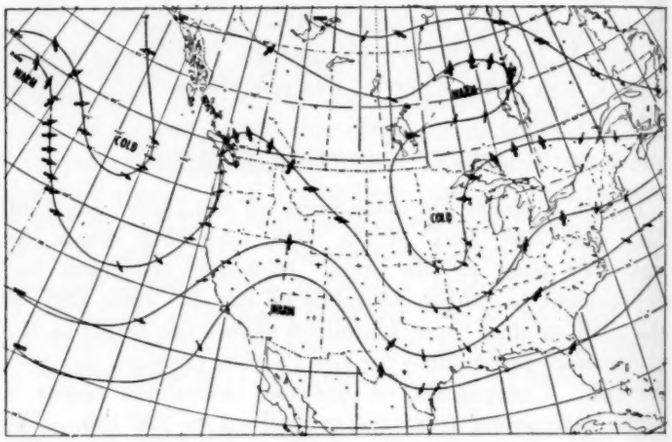

FIGURE 6.—Height-difference chart, 1000-700-mb., for 2200 EST, March 21, 1950. Height-difference (mean virtual temperature) lines at 200-ft. intervals are labeled in geopotential feet on the left and in degrees Centigrade on the right.

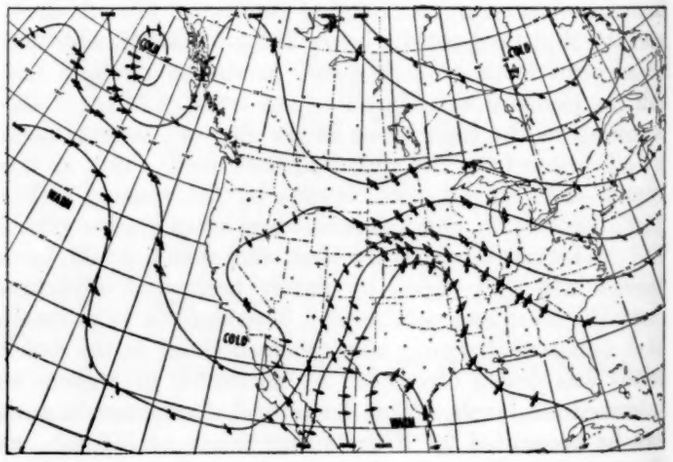

FIGURE 7.—Height-difference chart, 1000-700-mb., for 2200 EST, March 25, 1950. (See fig. 6 for explanation.)

small solid arrows show cold advection. Rough estimates of temperature advection can be made from these charts, though vertical motion, radiation, and other factors limit the accuracy of the results. Figure 6, the thickness chart for 2200 EST on the 21st, shows cold air over the central United States. During the succeeding four days, except for a short break with passage of a front on the 23d, there was continued warm advection over the Plains region, raising temperatures to the much higher values indicated in the thickness chart for 2200 EST, March 25 (fig. 7).

But as the Plains Low developed and deepened on the 25th and 26th, the very low surface pressure at the center resulted not only from high temperature in the lower troposphere, but also from the appearance over the center of warmer air aloft between the 300-mb. and 100-mb. levels, as may be seen by comparing the soundings taken over Omaha at 12-hour intervals (fig. 8). At the time of the sounding for 1000 EST of the 26th (fig. 8, solid line), Omaha was about 200 miles ahead of the surface cold front. This combined effect of the appearance of warmer air both at lower levels and aloft over deepening Lows has been described by Wulf and Obloy [4].

CHANGES IN THE UPPER TROPOSPHERE

A comparison between figure 9, the 500-mb. chart for 2200 EST, March 26, and figure 3, the corresponding chart 48 hours earlier, will illustrate some of the significant changes in the upper troposphere during development of the storm. The leading edge, CD, of the northwesterly winds moved forward about 1,200 miles and was still identified with the axis of cold air. In the same period, the leading edge, AB, of the very strong westerlies moved eastward about 1,100 miles. Figure 9 shows gradient wind speeds in excess of 100 knots in the region of strong gradient and slight anticyclonic curvature over eastern Texas. Since the average speed of the line AB was between 20 and 25 knots, the much higher speed of individual air parcels required that they move across the line and far to the east during the 48-hour period. These air parcels necessarily decelerated after crossing the line AB, because they encountered weaker gradient and were therefore deflected toward higher pressure, a factor contributing toward lowering of pressures, surface and aloft, in the vicinity of A. Thus some kinetic energy of the winds aloft was converted into potential energy within the storm area. This built-up potential energy, consisting of strong horizontal pressure gradient force, contributed in turn to the strong winds observed both at the surface and aloft, within the storm.

It is an interesting sidelight to note some further effects of the air parcels after they moved through the line AB of figure 9. Their trajectory took them at reduced but still high speeds (between 50 and 70 knots) across the ridge over the northeastern United States. At the time of

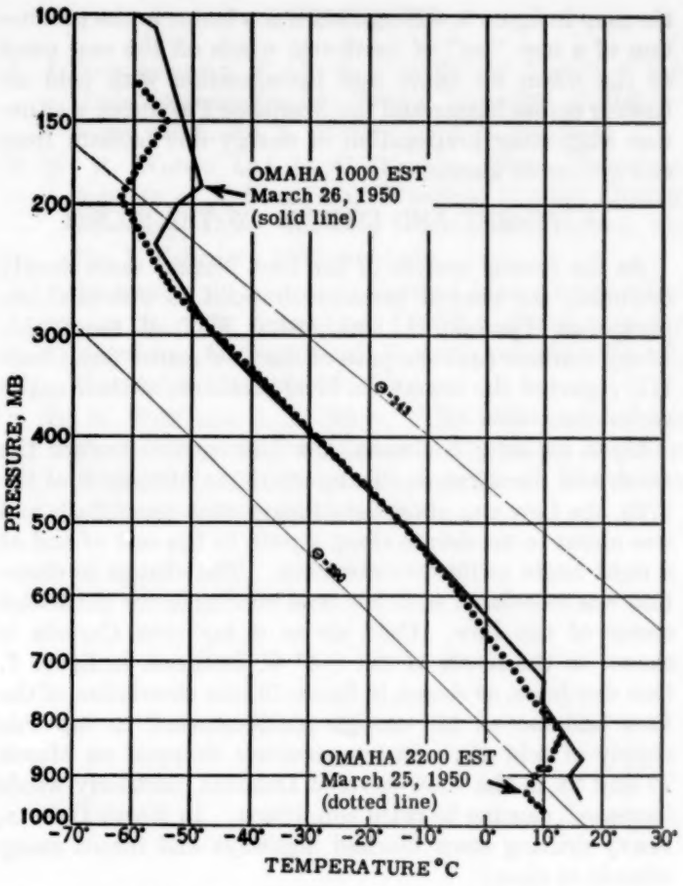

FIGURE 8.—Radiosonde observations from Omaha, Nebr.

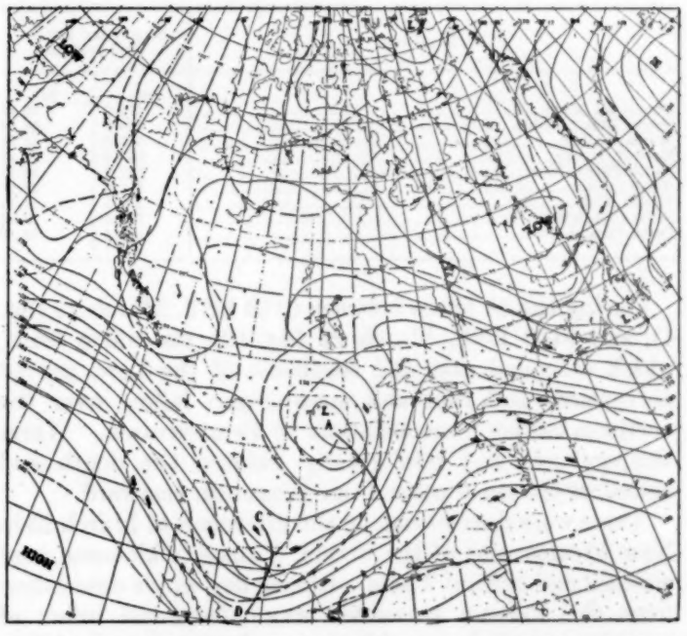

FIGURE 9.—500-mb. chart for 2200 EST, March 26, 1950. Contours (solid lines) at 200-ft. intervals are labeled in hundreds of geopotential feet. Isotherms (dashed lines) are drawn for intervals of 5° C. Winds are plotted in Beaufort scale.

the map in figure 9, this current was a factor in the production of a new "jet" of northwest winds off the east coast as the warm air came into juxtaposition with cold air flowing across Maine and the Maritime Provinces, a situation suggesting propagation of energy downstream from one system to another.

MOVEMENT AND EFFECTS OF THE STORM

As the frontal system of the Low became more deeply occluded, the central pressure dropped to 968 mb. (reported at Tyndall, S. Dak., 0130 EST of the 27th). Many stations near the path of the Low center (see Chart III) reported the lowest sea level pressures of their entire record (see table 1).

Upon entering Nebraska, the Low curved toward the north and decelerated. In figure 10, at 0130 EST of the 27th, the Low was almost stationary near Sioux Falls and was about to accelerate along a path to the east of and at a right angle to its previous path. The change in direction was associated with low level cooling in the northwest sector of the Low. Cold air as it lay over Canada is shown to the north of the −5° C. isotherm in figure 7. One day later, as shown in figure 10, the circulation of the Low had moved far enough northeastward to tap this supply of cold air. As temperatures dropped on March 27 and 28 in the snow-covered Dakotas, northerly winds increased, causing blizzard conditions. In North Dakota, heavy drifting snow blocked highways and forced many schools to close.

TABLE 1.—*List of new record low sea level pressures resulting from the storm of March 25–27, 1950*

W. B. station	New record low sea level pressure	
	mb.	*in.*
Concordia, Kans.	972.9	28.73
Grand Island, Nebr.	969.9	28.64
Huron, S. Dak.	970.5	28.66
Norfolk, Nebr.	970.9	28.67
North Platte, Nebr.	972.2	28.71
Omaha, Nebr.	973.9	28.76
Pueblo, Colo.	976.6	28.84
Sioux City, Iowa	970.5	28.66
Sioux Falls, S. Dak.	969.5	28.63

During the 48 hours between 0130 EST, March 25 (fig. 4), and 0130 EST, March 27 (fig. 10), the warm front, which extended east and southeast of the Low, moved northward, and rain and snow began falling over the northern States from Montana to Pennsylvania. Warm temperatures and rain greatly reduced the depth and extent of the snow cover from Wisconsin eastward.

There were dust storms on the afternoon of March 25 in New Mexico east of the divide, Kansas, Oklahoma, and western and central Texas. Strong dry winds descending from the Plateau prevented any substantial influx of maritime tropical air, with the result that no rain fell in that area during the progress of the storm. This section had received almost no rain for 6 weeks, and the amount

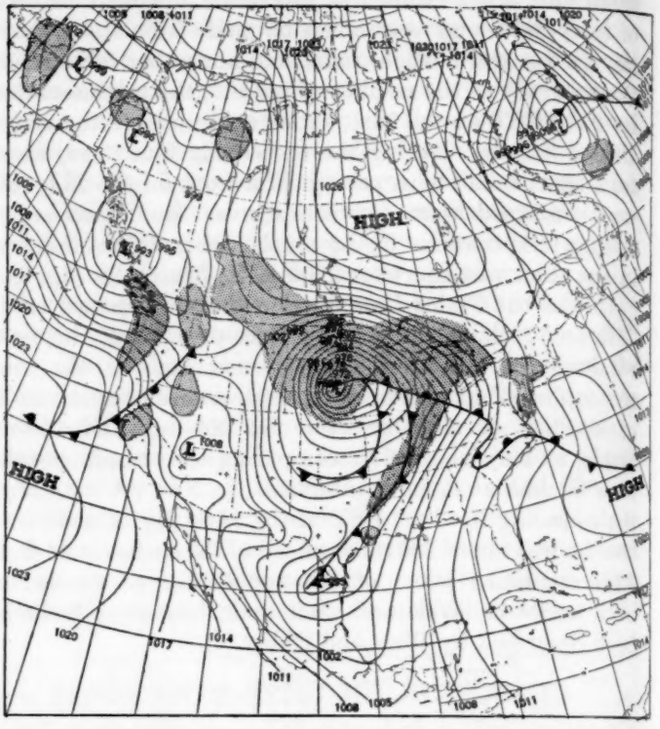

FIGURE 10.—Surface weather map for 0130 EST, March 27, 1950. Shading indicates areas of active precipitation.

during the entire winter was far below normal. Wind speeds generally were more than 40 miles per hour and some stations reported winds up to 70 miles per hour for short periods. Temperature-dew point differences were as much as 60° to 80° F.; at Lamar, Colo., a temperature of 79° F. was reported with a dew point of −8° F. Great quantities of rich top soil were blown away. Soil damage and drought caused some farmers, particularly in western Oklahoma, to abandon fields planted to small grains.

The main cold front of the storm passed Albuquerque during the afternoon of the 25th. The dust storm was intensified by rapidly moving turbulent air just behind the front, causing dust to be lifted to higher levels and to be carried far to the east, including the southeastern part of the country where the cold front was also accompanied by considerable severe weather.

On the afternoon of the 26th, when the cold front approached the deep flow of maritime tropical air over Missouri, Arkansas, and extreme eastern Texas, thunderstorm and shower activity broke out in the warm moist air. At the time of the map shown in figure 10, 0130 EST of the 27th, the heaviest rainfall was occurring near the main cold front from LaCrosse through St. Louis and Little Rock to Houston. As the front moved eastward, rain amounts of more than 2 inches were reported in a band from Little Rock to Indianapolis, and lesser amounts to the east and south. Much of this precipitation fell

from thunderstorms along the cold front, but many prefrontal thunderstorms broke out in Illinois and Indiana on the night of the 26th.

Several tornadoes were reported ahead of the cold front as it passed through Arkansas, Louisiana, and Mississippi. In Mississippi, property damage amounted to several hundred thousand dollars. Gusts up to 100 miles per hour were reported at the Jackson, Miss., Airport. Some further wind damage was reported as the front and accompanying thunderstorms moved across Alabama.

By 0130 EST of March 28th, a new Low center formed along the occluded front just north of Lake Huron. During the next 12 hours, the original Low center filled as it crossed northern Wisconsin. At the same time the main cold front passed off the east coast into the Atlantic, and a few snow flurries in the North Central States were all that remained of the weather produced by the storm.

REFERENCES

1. J. Namias and P. F. Clapp, "Confluence Theory of the High Tropospheric Jet Stream," *Journal of Meteorology*, vol. 6, No. 5, October 1949, p. 330–336.
2. H. B. Wobus and L. C. Norton, "Some Synoptic Aspects of a Change in Weather Regime During February, 1950," *Monthly Weather Review*, vol. 78, No. 2, February 1950, p. 31–40.
3. J. Vederman, "Changes in Vertical Mass Distribution over Rapidly Deepening LOWS," *Bulletin of the American Meteorological Society*, vol. 30, No. 9, November 1949, p. 303–309.
4. O. R. Wulf and S. J. Obloy, "The Utilization of the Entire Course of Radiosonde Flights in Weather Diagnosis," *Miscellaneous Reports*, No. 10, University of Chicago Press, 1944, p. 7.

885753—50——2

U. S. GOVERNMENT PRINTING OFFICE: 1950

Chart I. Departure (°F.) of the Mean Temperature from the Normal, and Wind Roses for Selected Stations, March 1950

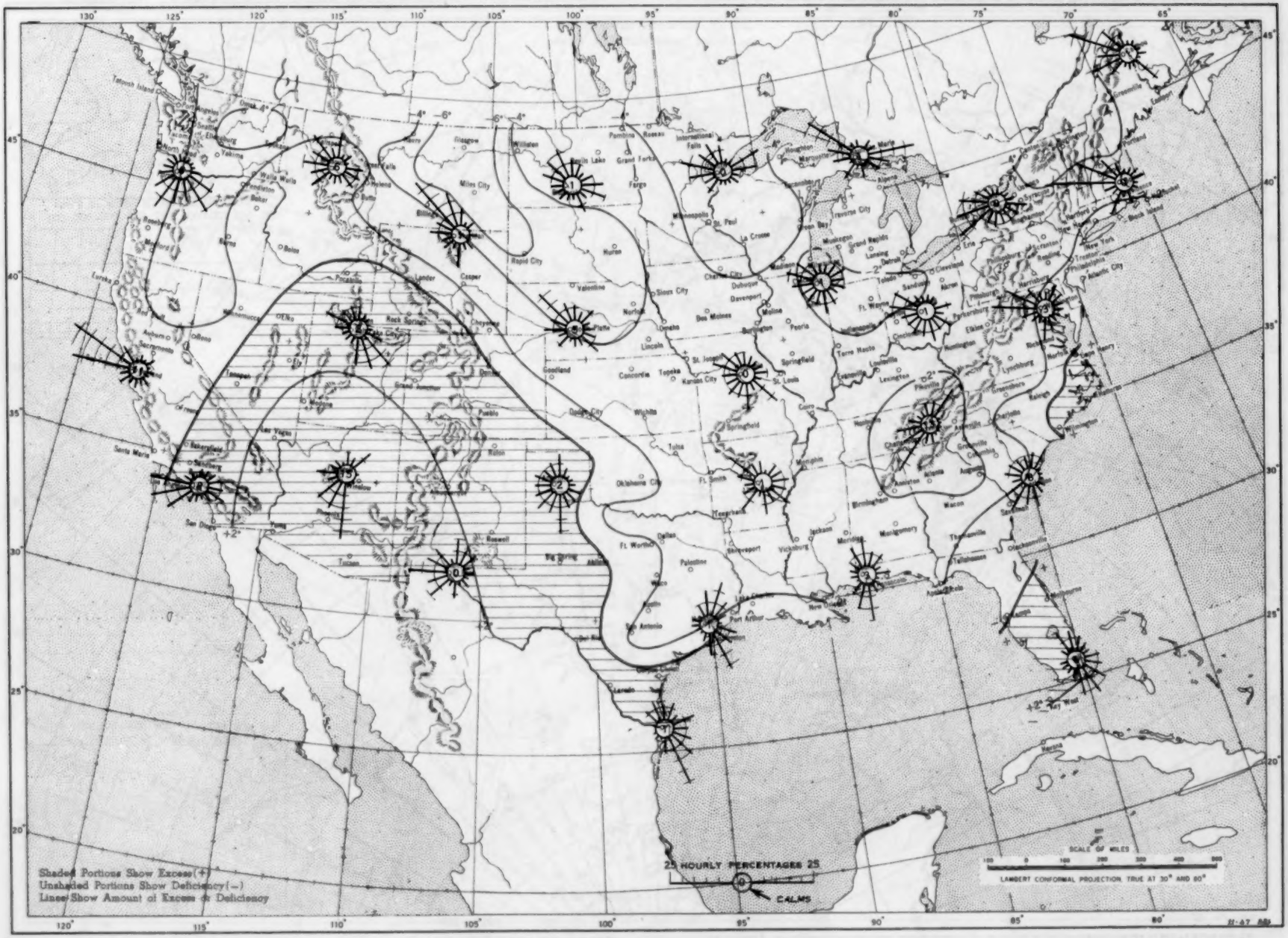
Shaded Portions Show Excess (+)
Unshaded Portions Show Deficiency (−)
Lines Show Amount of Excess or Deficiency
25 HOURLY PERCENTAGES 25
CALMS
SCALE OF MILES
LAMBERT CONFORMAL PROJECTION TRUE AT 30° AND 60°

Chart II. Tracks of Centers of Anticyclones, March 1950. (Inset) Departure of Monthly Mean Pressure from Normal

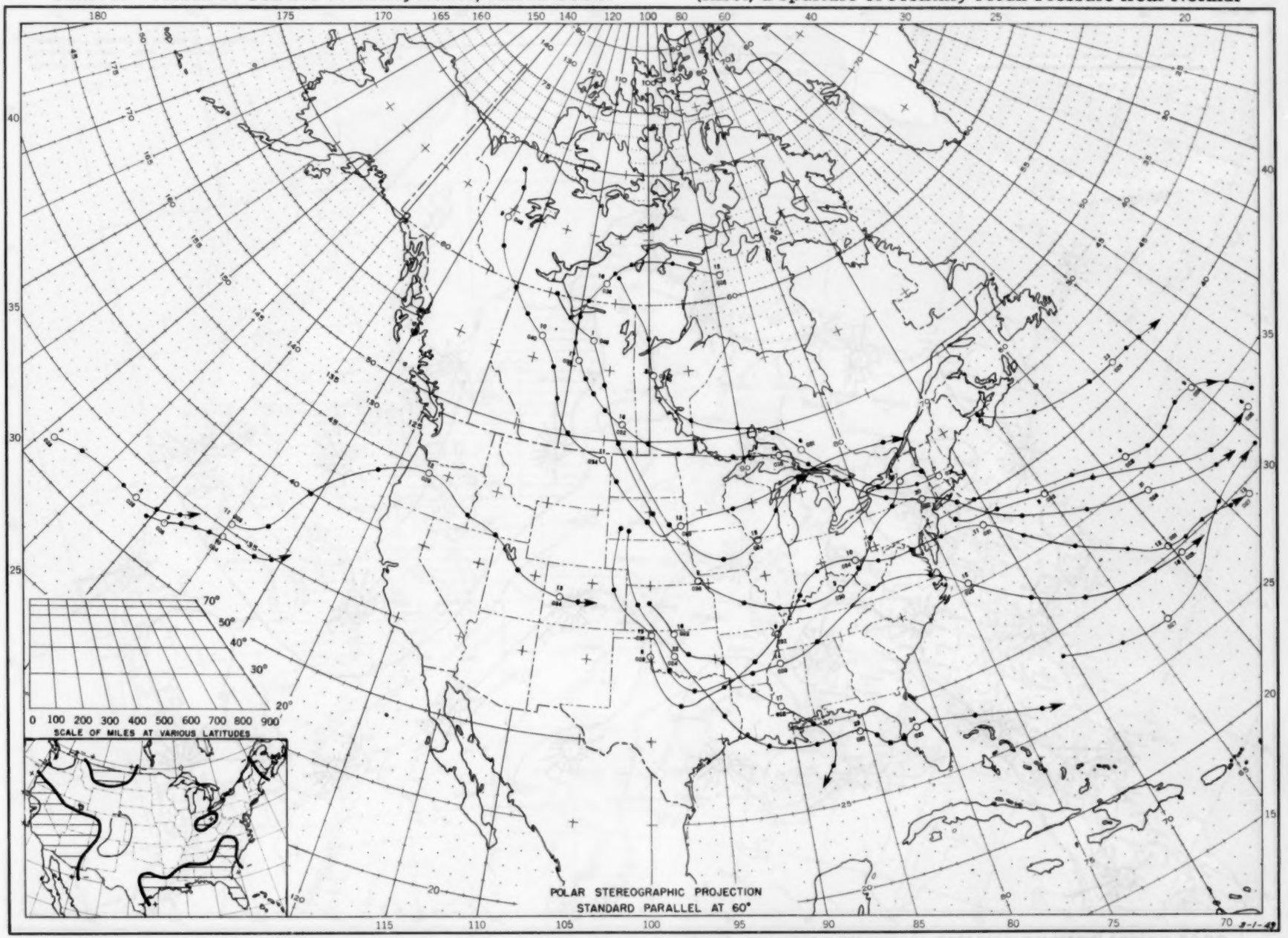

Circle indicates position of anticyclone at 7:30 a. m. (75th meridian time). Dots indicate intervening 6-hourly positions. Figure above circle indicates date, and figure below, pressure to nearest millibar. Only those centers which could be identified for 24 hours or more are included.

Chart III. Tracks of Centers of Cyclones, March 1950. (Inset) Change in Mean Pressure from Preceding Month

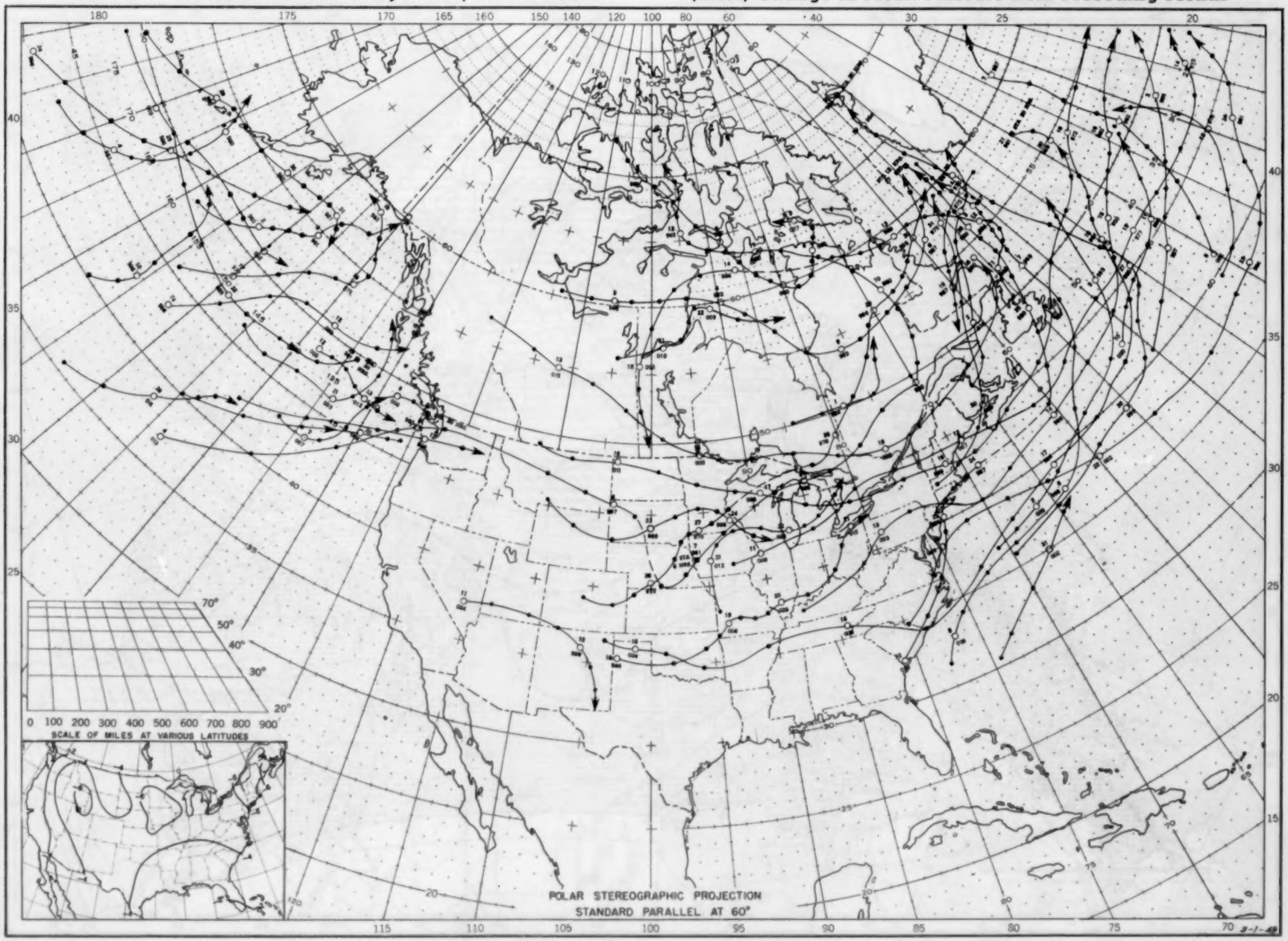

Circle indicates position of cyclone at 7:30 a. m. (75th meridian time) Dots indicate intervening 6-hourly positions. Figure above circle indicates date, and figure below, pressure to nearest millibar. Only those centers which could be identified for 24 hours or more are included.

Chart IV. Percentage of Clear Sky Between Sunrise and Sunset, March 1950

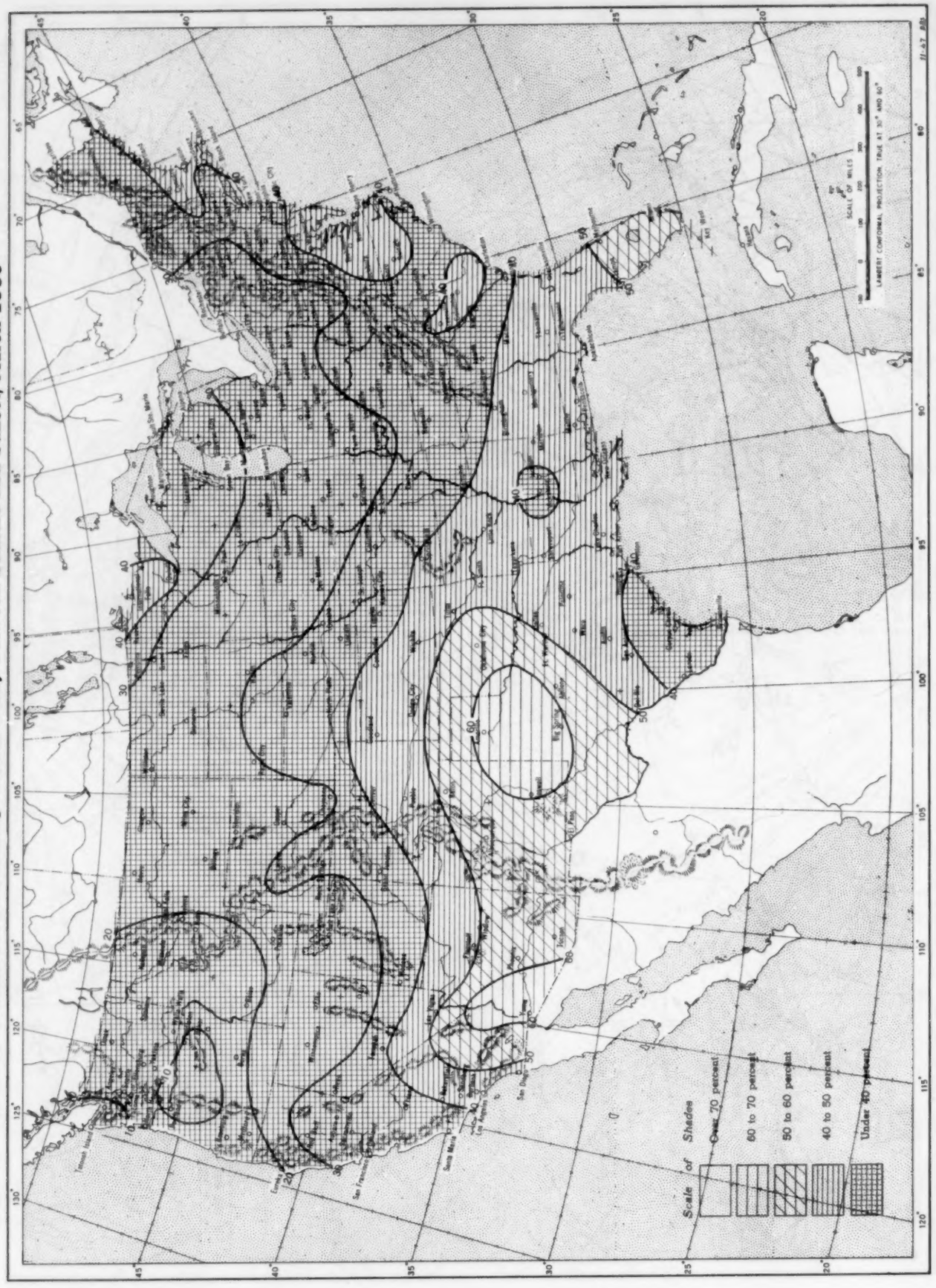
Scale of Shades
Over 70 percent
60 to 70 percent
50 to 60 percent
40 to 50 percent
Under 40 percent
LAMBERT CONFORMAL PROJECTION, TRUE AT 30° AND 60°
SCALE OF MILES

Chart V. Total Precipitation, Inches, March 1950. (Inset) Departure of Precipitation from Normal

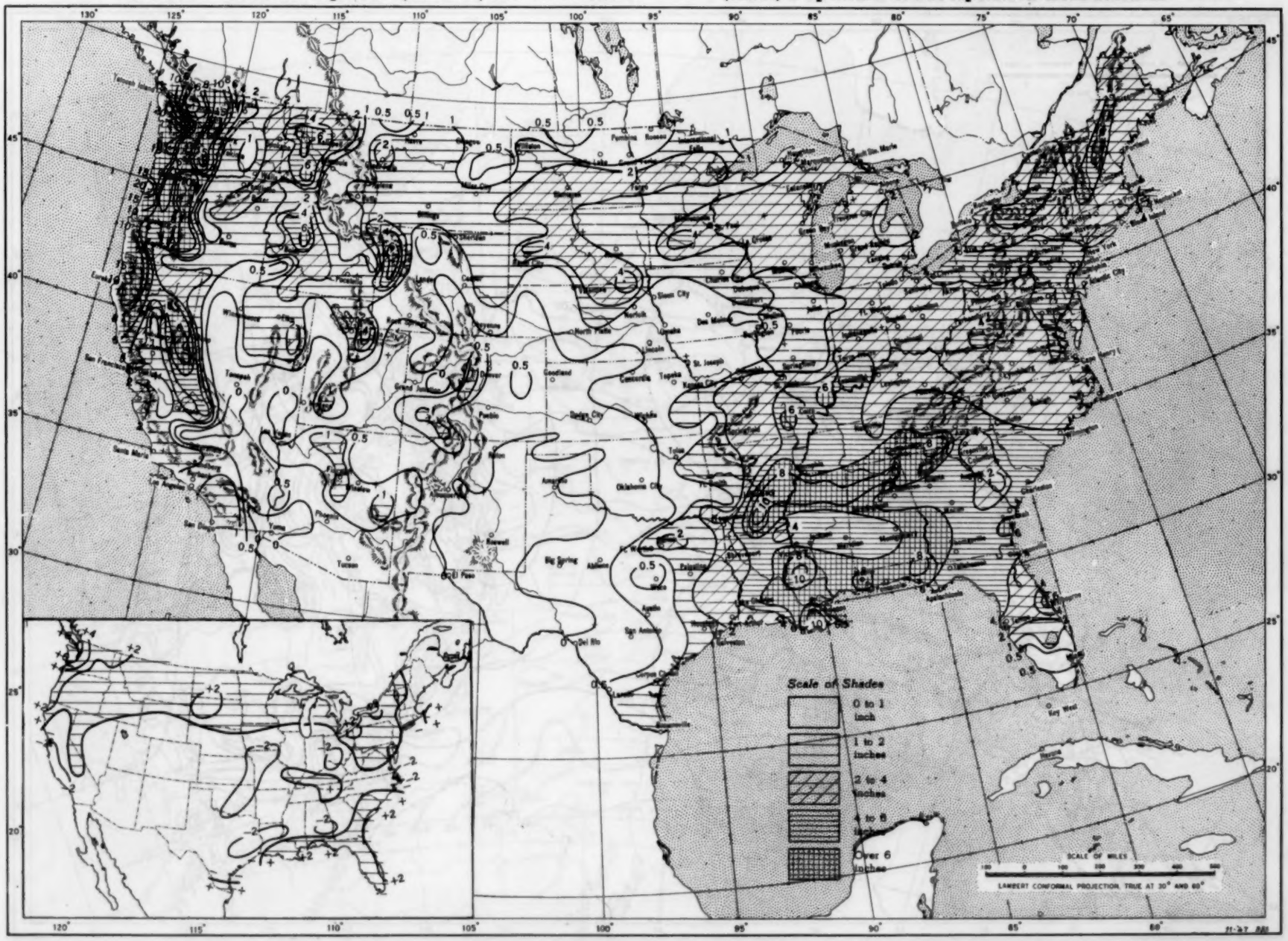
Scale of Shades
0 to 1 inch
1 to 2 inches
2 to 4 inches
4 to 6 inches
Over 6 inches
SCALE OF MILES
LAMBERT CONFORMAL PROJECTION, TRUE AT 30° AND 60°

Chart VI. Mean Isobars (mb.) at Sea Level and Mean Isotherms (°F.) at Surface., March 1950

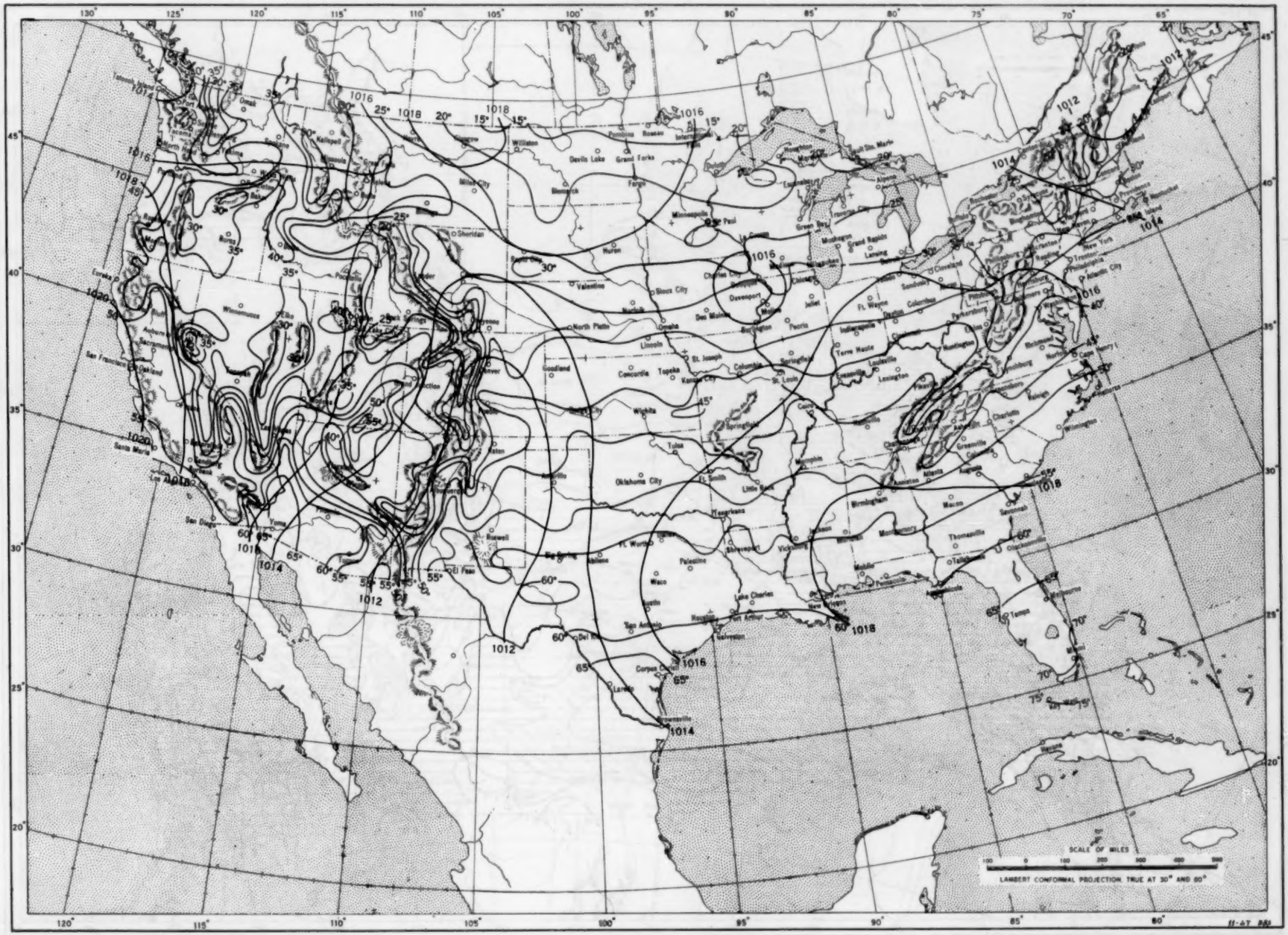

Chart VII. Total Snowfall, Inches, March 1950. (Inset) Depth of Snow on the Ground at 7:30 a. m., March 28, 1950

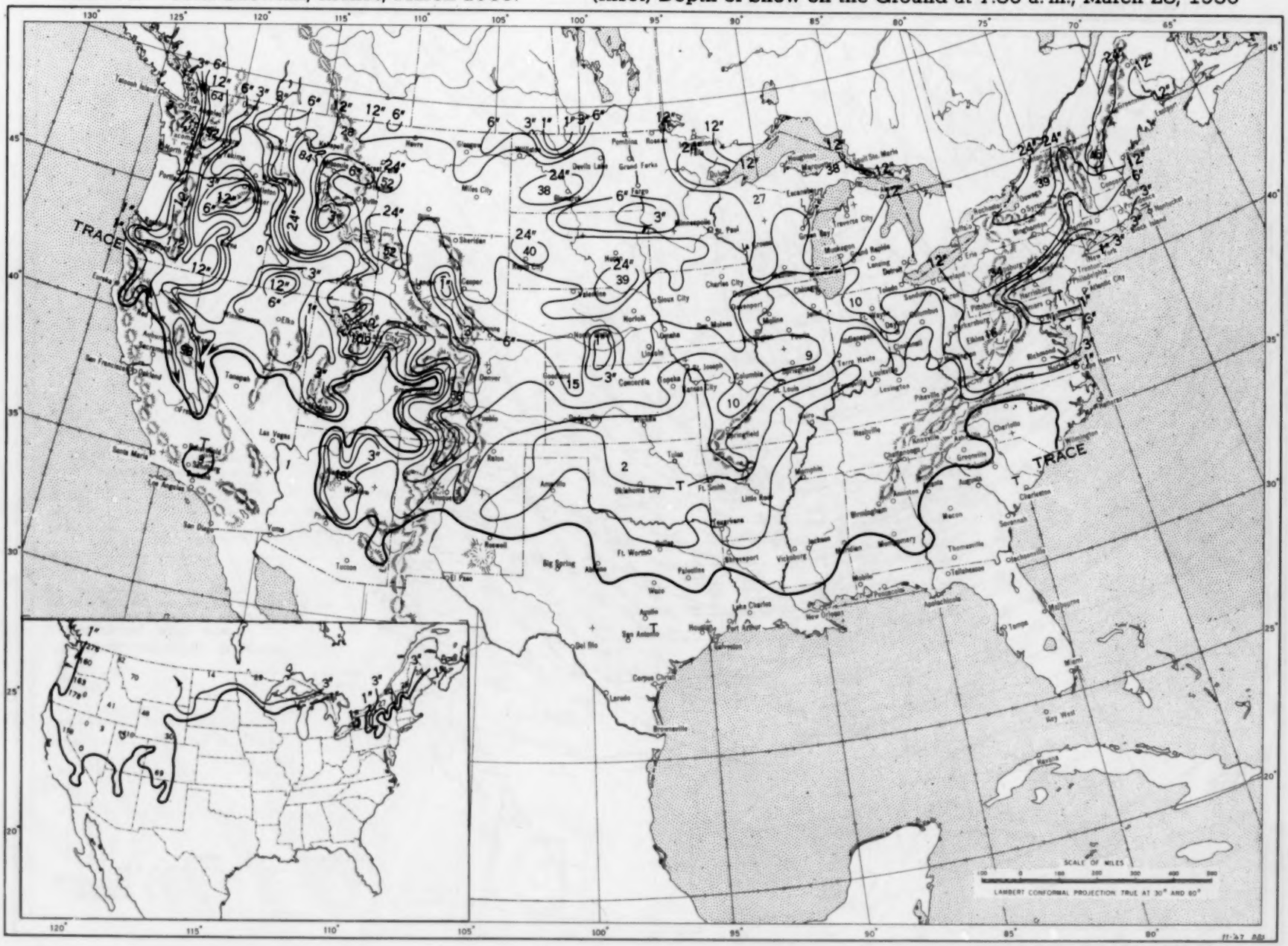

Chart VIII, March 1950. Contour Lines of Mean Dynamic Height (Geopotential) in Units of 0.98 Dynamic Meters and Mean Isotherms in Degrees Centigrade for the 850-millibar Pressure Surface, and Resultant Winds at 1,500 Meters (m. s. l.)

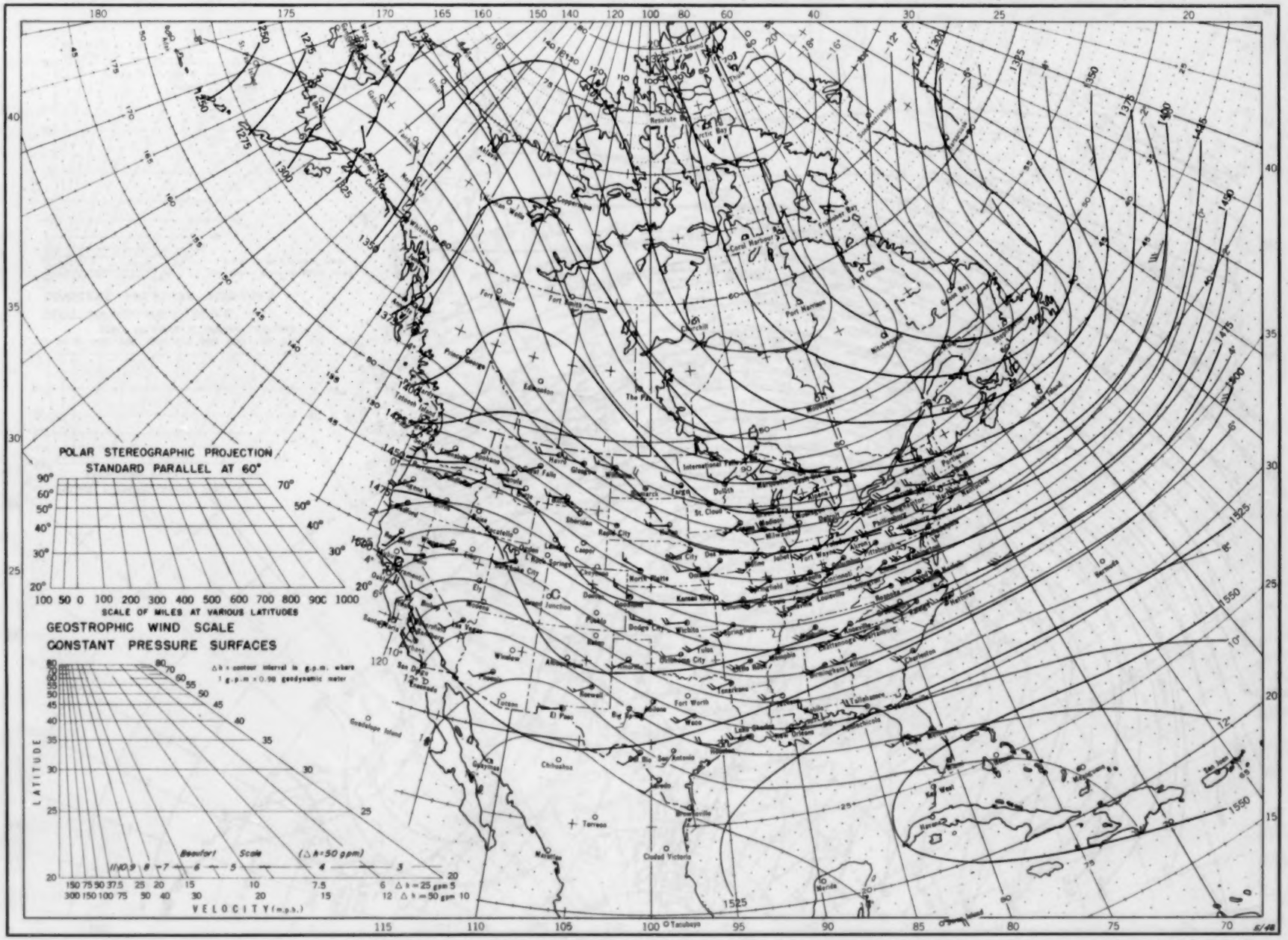

Contour lines and isotherms based on radiosonde observations at 0300 G. C. T. Winds indicated by black arrows based on pilot balloon observations at 2100 G. C. T.; those indicated by red arrows based on rawins taken at 0300 G. C. T.

Chart IX, March 1950. Contour Lines of Mean Dynamic Height (Geopotential) in Units of 0.98 Dynamic Meters and Mean Isotherms in Degrees Centigrade for the 700-millibar Pressure Surface, and Resultant Winds at 3,000 Meters (m. s. l.)

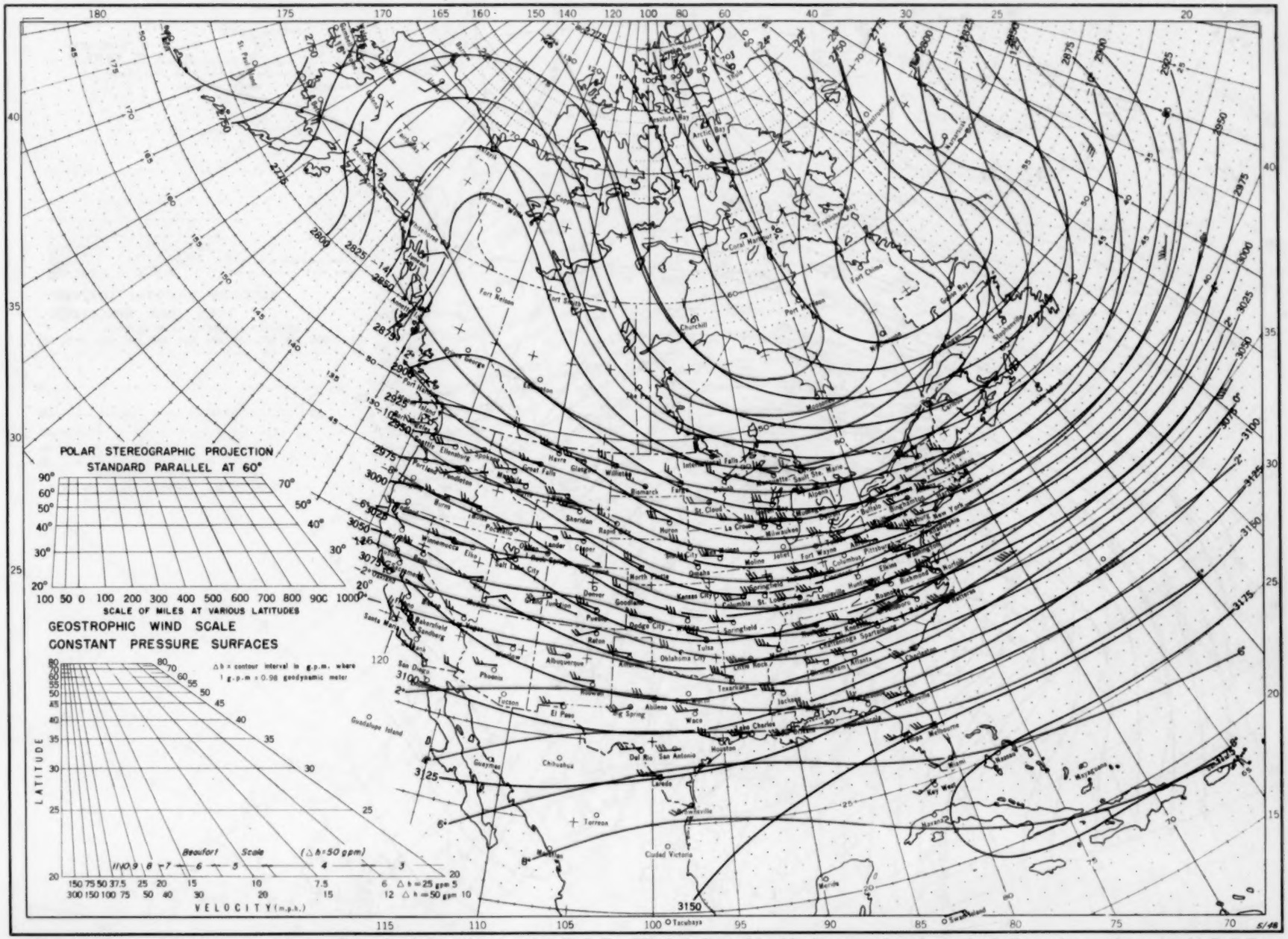

Contour lines and isotherms based on radiosonde observations at 0300 G. C. T. Winds indicated by black arrows based on pilot balloon observations at 2100 G. C. T.; those indicated by red arrows based on rawins taken at 0300 G. C. T.

Chart X, March 1950. Contour Lines of Mean Dynamic Height (Geopotential) in Units of 0.98 Dynamic Meters and Mean Isotherms in Degrees Centigrade for the 500-millibar Pressure Surface, and Resultant Winds at 5,000 Meters (m. s. l.)

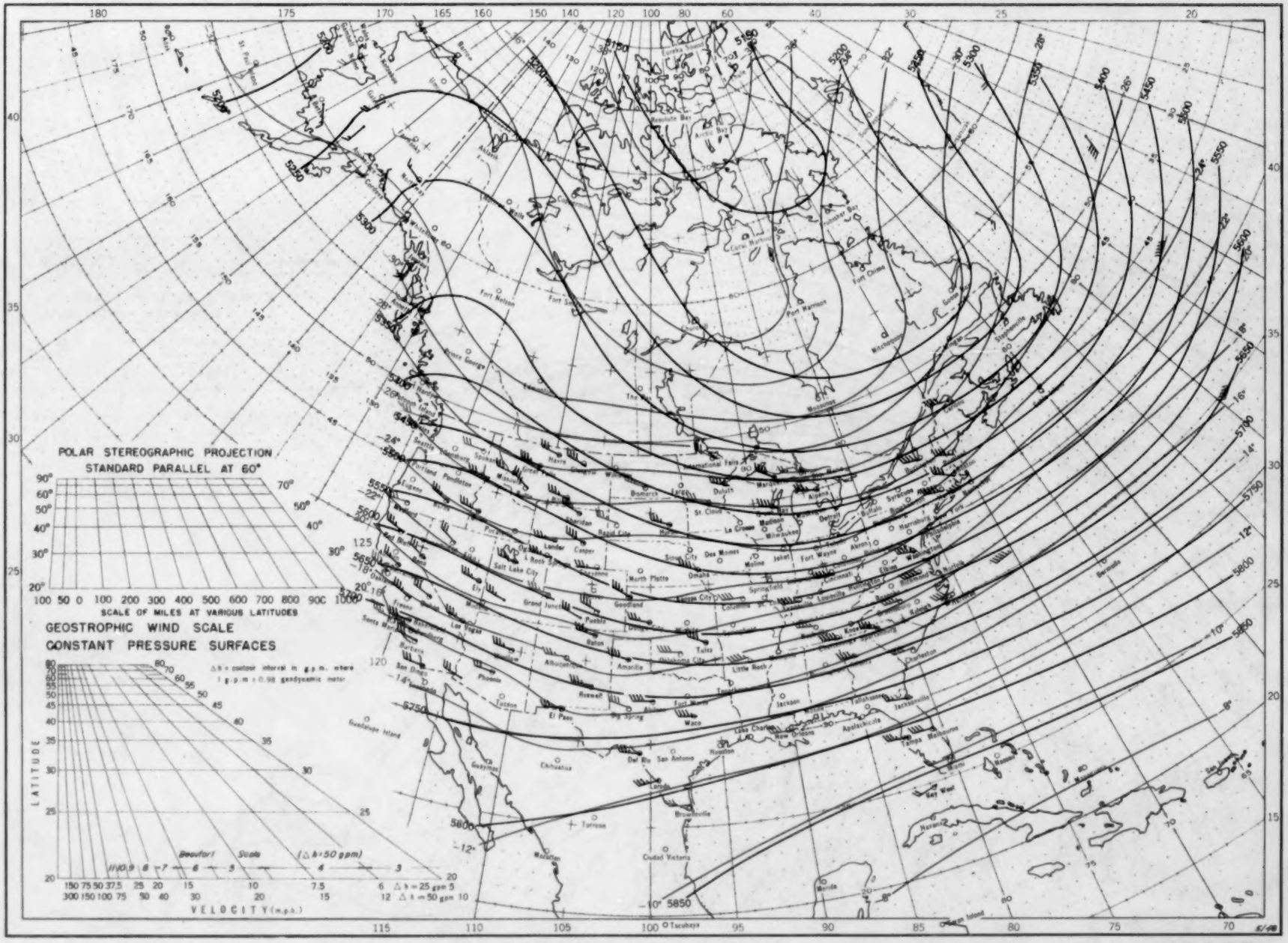

Contour lines and isotherms based on radiosonde observations at 0300 G. C. T. Winds indicated by black arrows based on pilot balloon observations at 2100 G. C. T.; those indicated by red arrows based on rawins taken at 0300 G. C. T.

Chart XI, March 1950. Contour Lines of Mean Dynamic Height (Geopotential) in Units of 0.98 Dynamic Meters and Mean Isotherms in Degrees Centigrade for the 300-millibar Pressure Surface, and Resultant Winds at 10,000 Meters (m. s. l.)

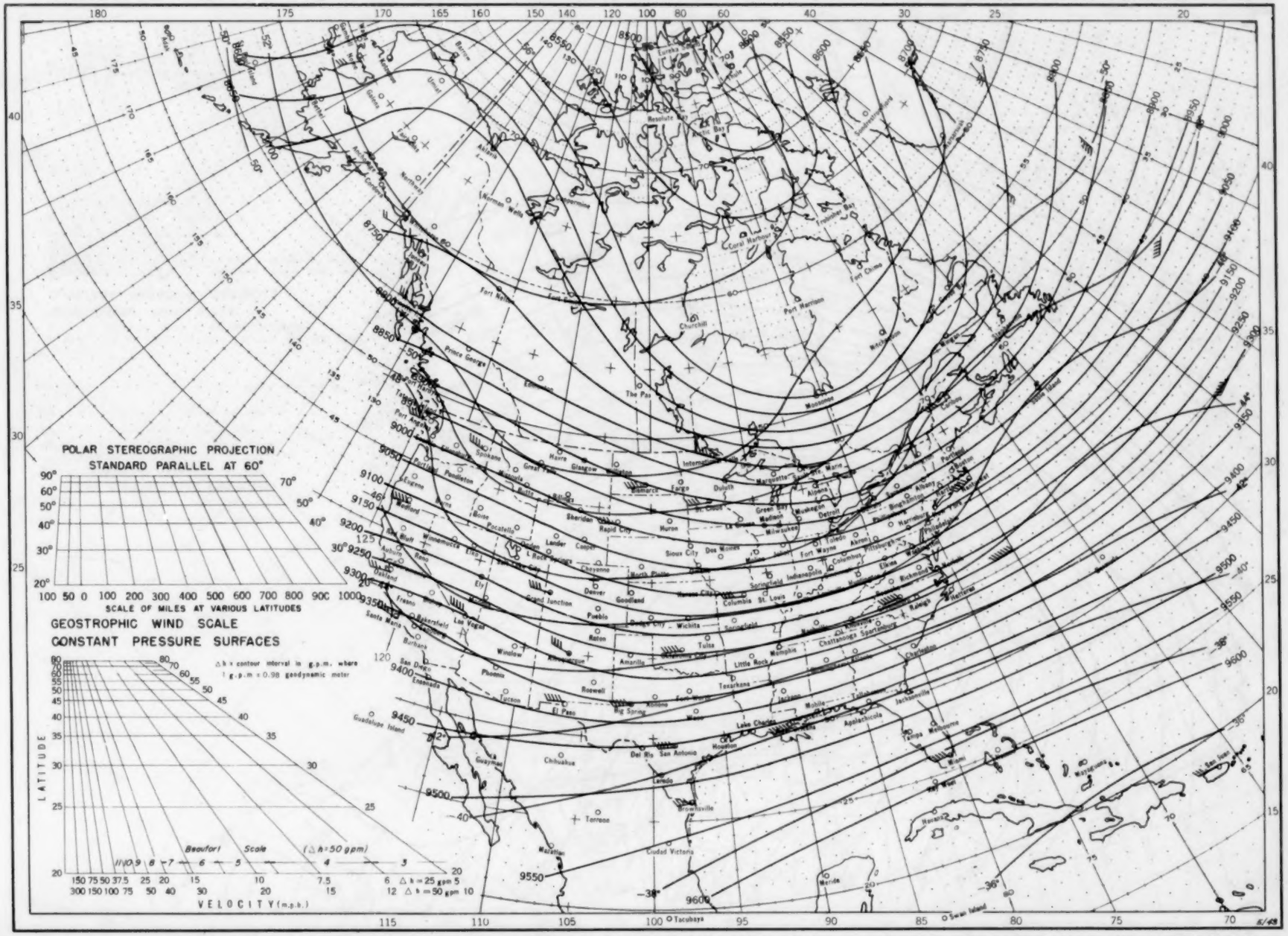
POLAR STEREOGRAPHIC PROJECTION
STANDARD PARALLEL AT 60°
SCALE OF MILES AT VARIOUS LATITUDES
GEOSTROPHIC WIND SCALE
CONSTANT PRESSURE SURFACES
LATITUDE
VELOCITY (m.p.h.)
Beaufort Scale
Δh = contour interval in g.p.m. where 1 g.p.m. = 0.98 geodynamic meter

Contour lines and isotherms based on radiosonde observations at 0300 G. C. T. Winds indicated by black arrows based on pilot balloon observations at 2100 G. C. T.; those indicated by red arrows based on rawins taken at 0300 G. C. T.